Magnetic sensors: from ultrathin film growth to sensor integration in unexpected systems

Susana Cardoso de Freitas

Group leader Spintronics & Magnetic Sensors

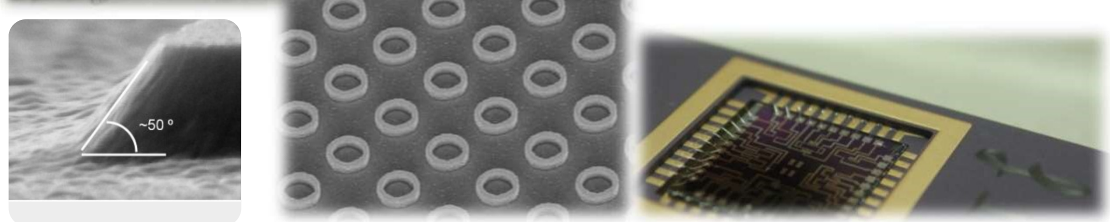

INESC – Microsystems and Nanotechnologies
Lisbon, Portugal
www.inesc-mn.pt

Outline

INESC MN
Microsistemas & Nanotecnologias

Magnetoresistive sensors

- thin film materials
- thermal stability
- noise, SNR => detectivity for pT
- 3D detection on chip

Applications

Magnetic sensors

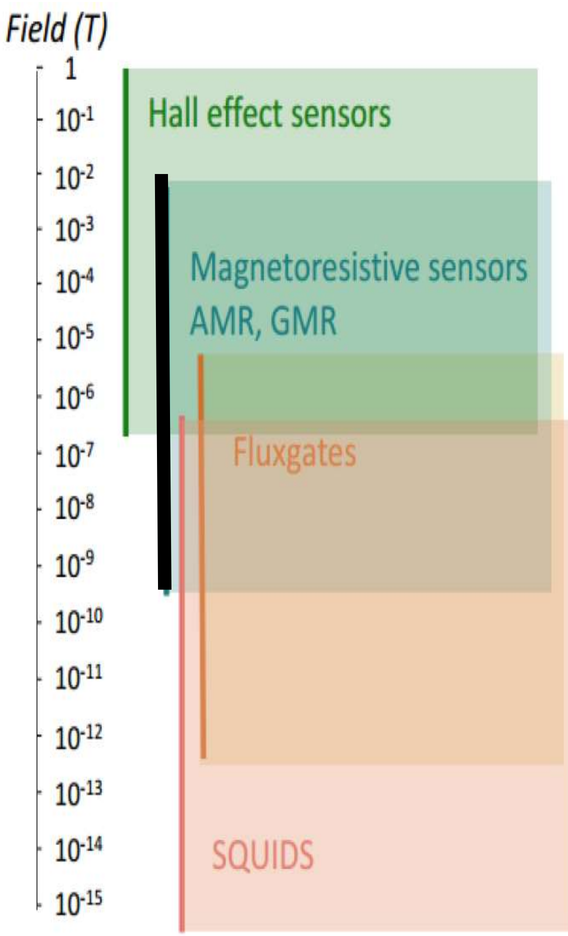

Hall effect
- Low spatial resolution
- Low sensitivity
- Operating temperature: Room temperature

xMR
- High spatial resolution
- High sensitivity
- Operating temperature: Room temperature

xMR sensors

Fluxgates
- Low spatial resolution
- High sensitivity
- Operating temperature: Room temperature

SQUIDS
- Low spatial resolution
- High sensitivity
- Operating temperature: Cryogenic temperature

WHY MAGNETORESISTIVE SENSORS ARE CANDIDATES FOR MANY APPLICATIONS ?

INESC MN
Microsistemas & Nanotecnologias

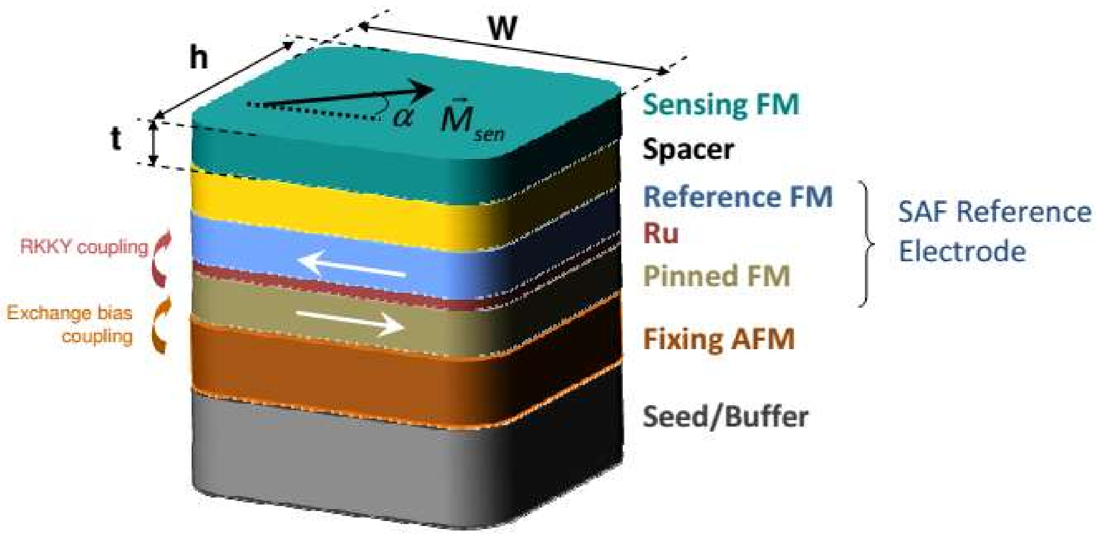

Magnetoresistance

$$\mathrm{MR} = \frac{R_{max} - R_{min}}{R_{min}}$$

AMR: 2-5%
GMR: 6~15%
Al_2O_3 TMR: 20~40%
MgO TMR: 80~260%

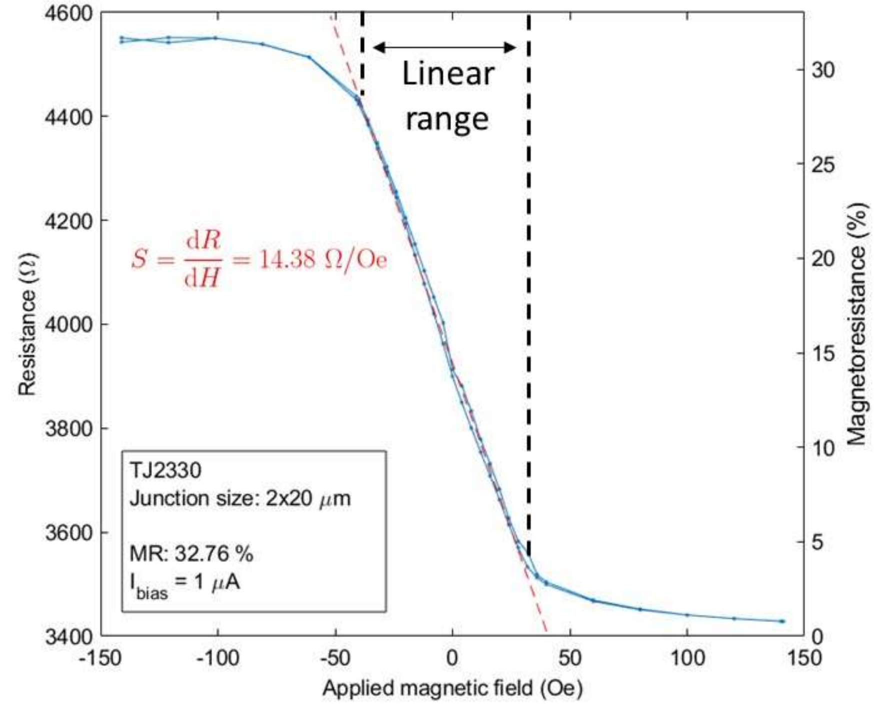

Linear range

ΔH ~ 10-300 Oe

(1-30 mTesla)

Magnetic tunnel junction - TMR

INESC MN
Microsistemas & Nanotecnologias

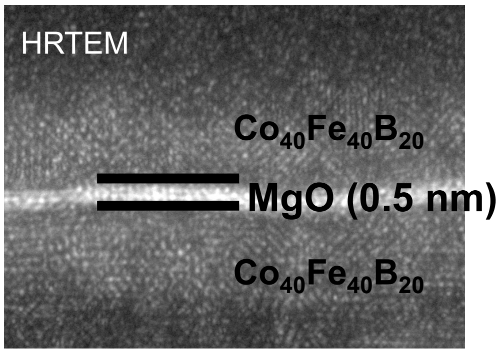

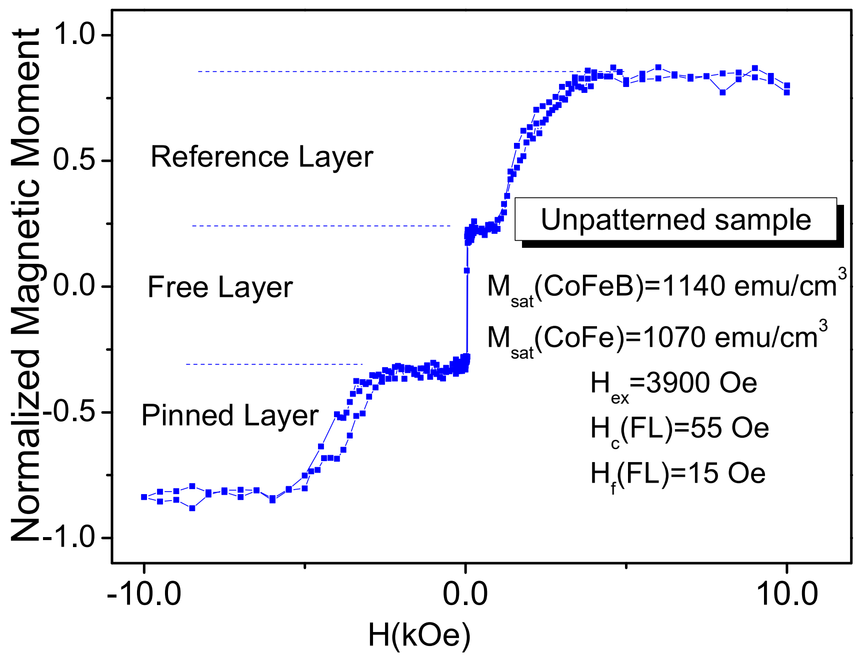

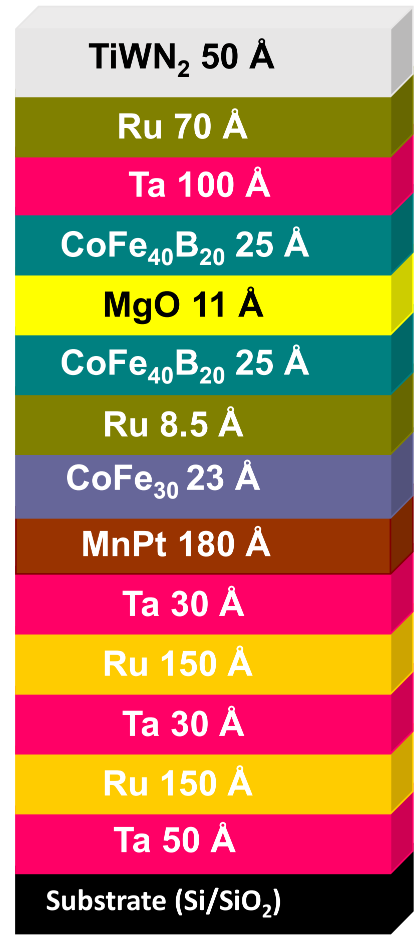

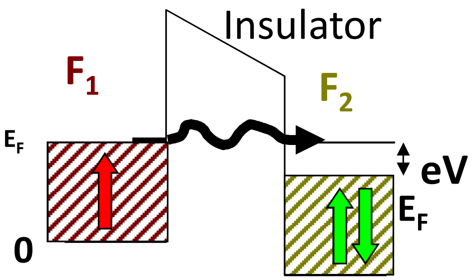

MIT, 1996
IBM, 1997
INESC, 1997

Electrons will tunnel if apply voltage between electrodes
Spin is conserved upon tunneling

Accurate control of the thin film thickness

- impact on TMR
- impact on R

INESC MN
Microsistemas & Nanotecnologias

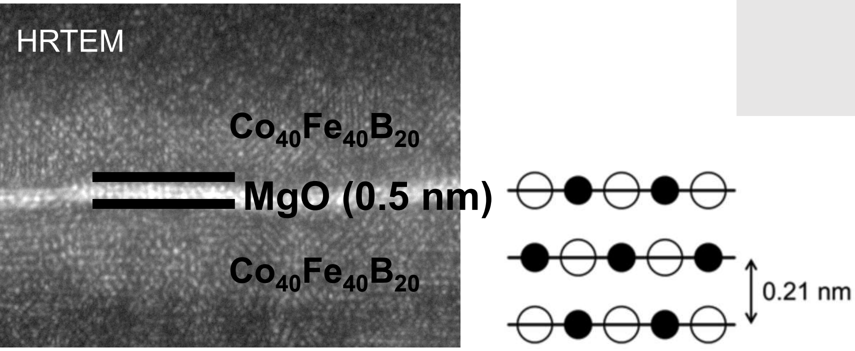

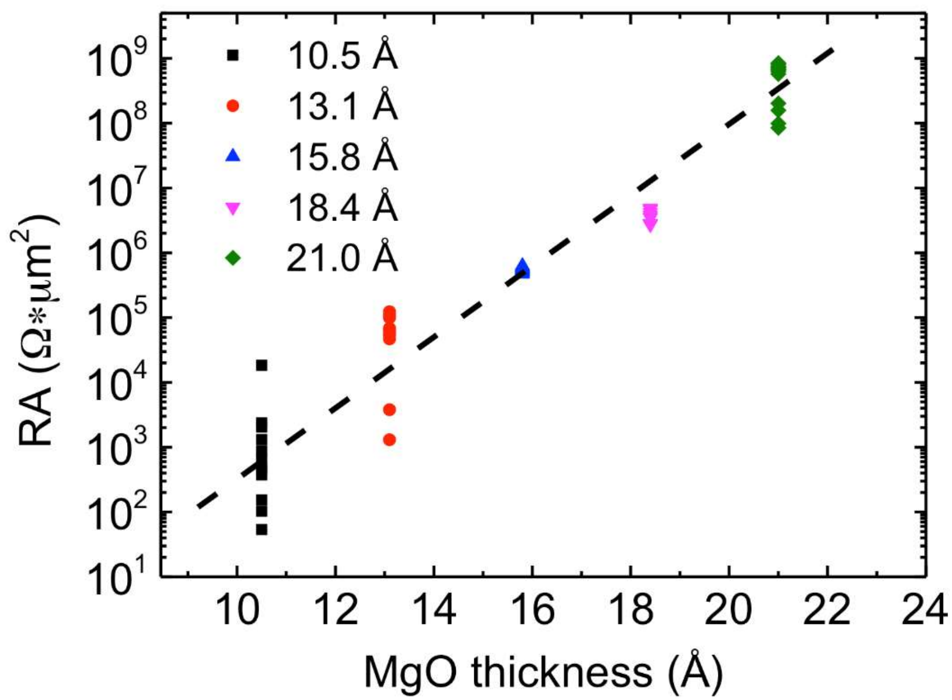

1 Å => 10x R

Micromagnetic and Analytical Models

INESC MN
Microsistemas & Nanotecnologias

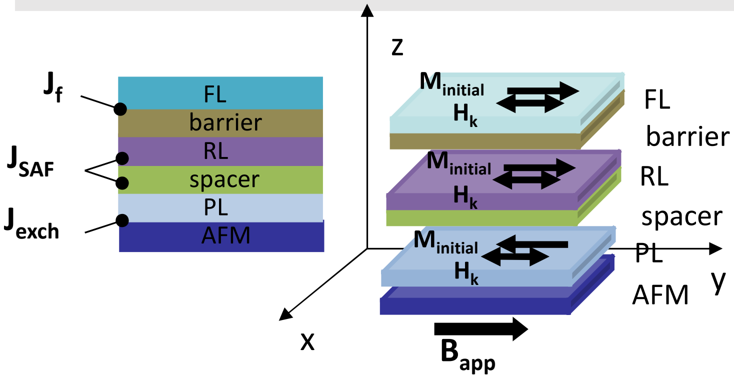

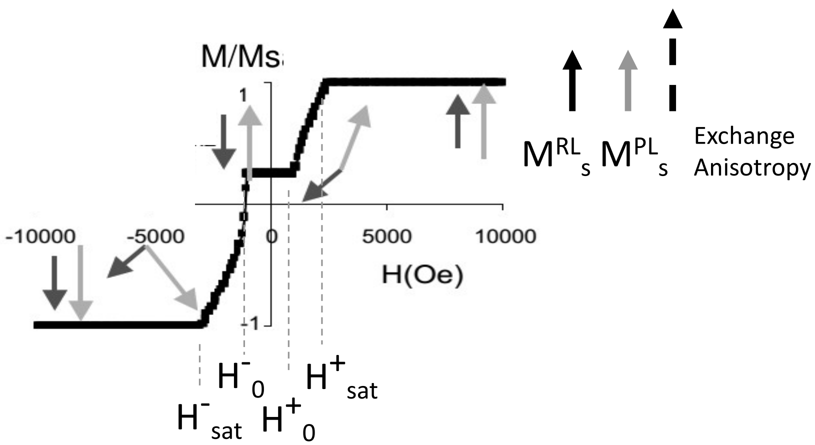

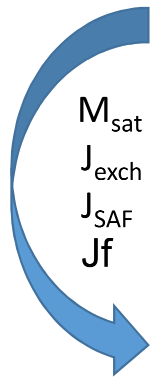

Experimental

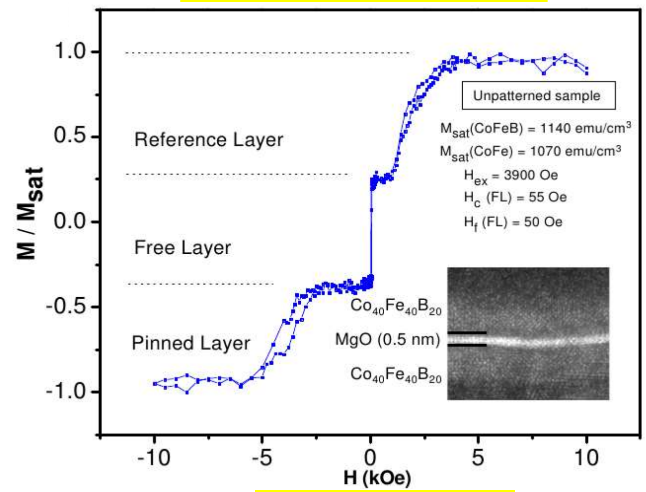

Simulation

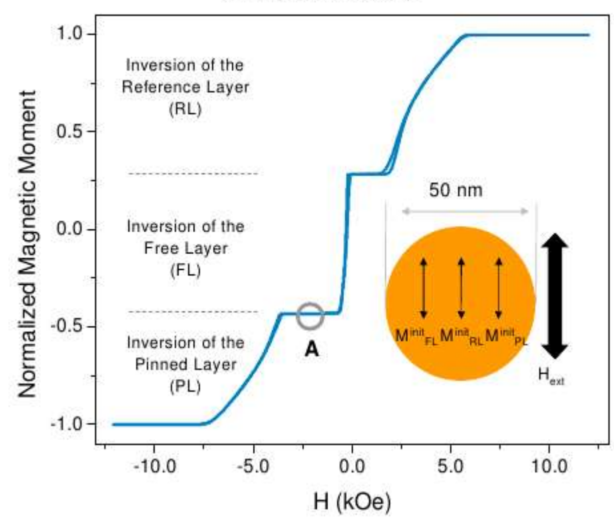

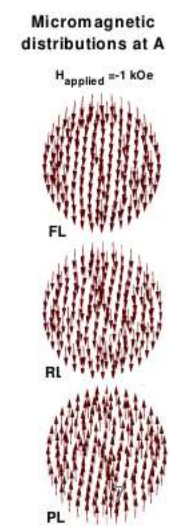

Magnetoelectronics, Elsevier, Ed. Mark Jonhson, 2004

IEEE Trans.Magn.49 (7), pp. 4405-4408 (2013

Nanotechnology 27, 045501 (2015)

Physica B: Cond. Matter, 435, 163 (2014)

Scientific Reports , 11, 215 (2021)

Appl.Phys.Letters **118**, 072401 (2021);

Adv. Electronic Materials, 7 , 2000976 (2020)

IEEE Magn.Mat. (in press, 2023)

INESC MN
Microsistemas & Nanotecnologias

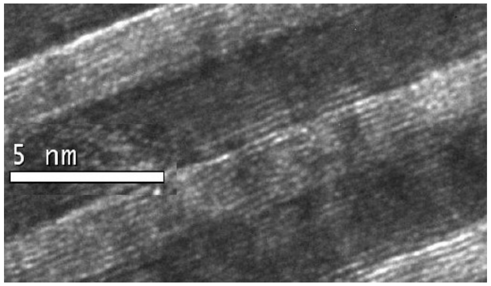

Film thickness:
Controlled at the atomic scale
1 Å = 0.1 nm

Multilevel device patterning

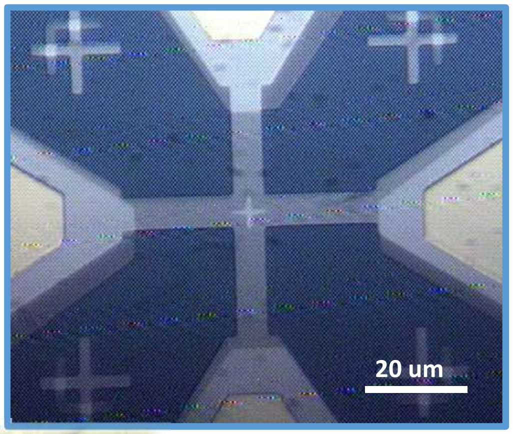

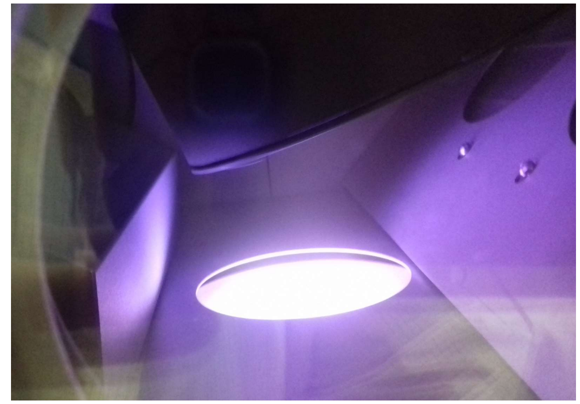

MgO target with Ar plasma

Wafer microfabrication in a Clean Room

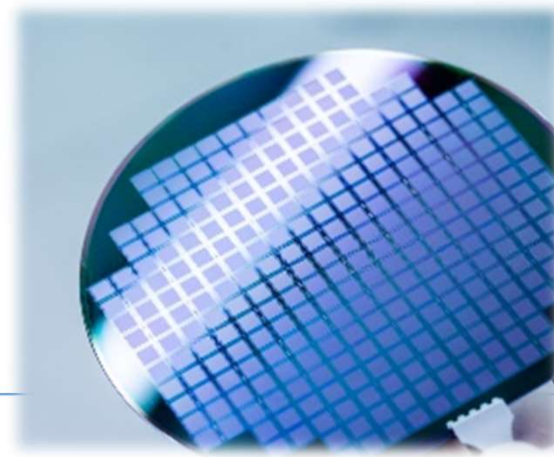

INESC MN
Microsistemas &
Nanotecnologias

Challenges II

Low noise, high signal

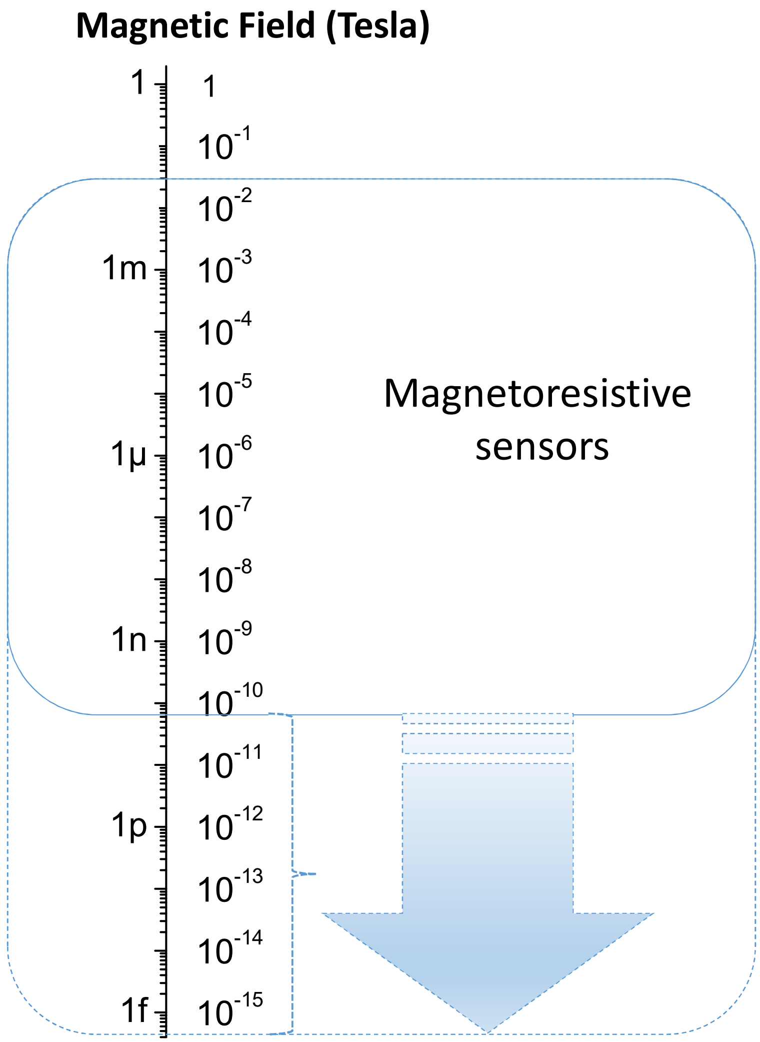
Magnetic Field (Tesla)
1
1m
1μ
1n
1p
1f
1
10-1
10-2
10-3
10-4
10-5
10-6
10-7
10-8
10-9
10-10
10-11
10-12
10-13
10-14
10-15
Magnetoresistive sensors

How to distinguish signal from noise ?

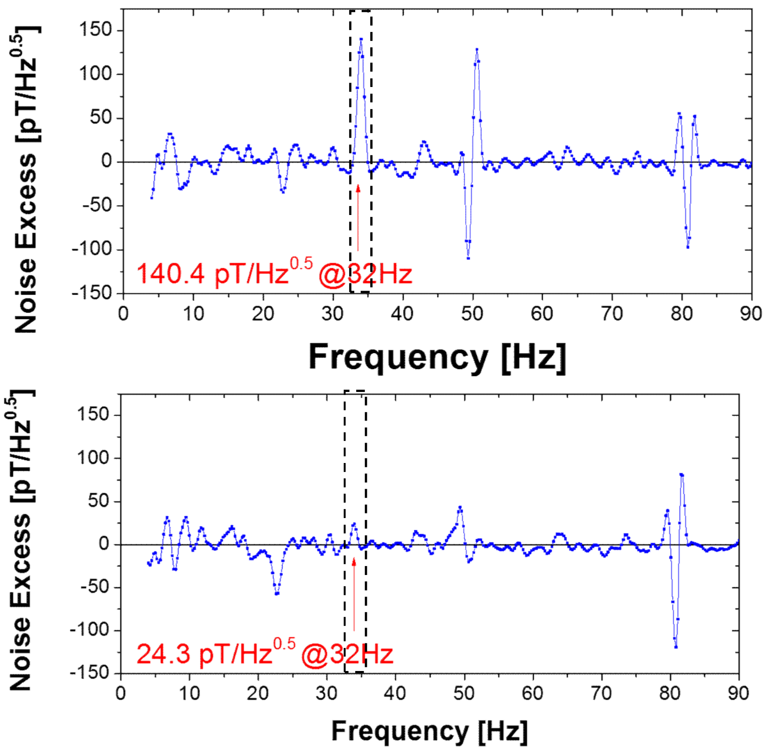

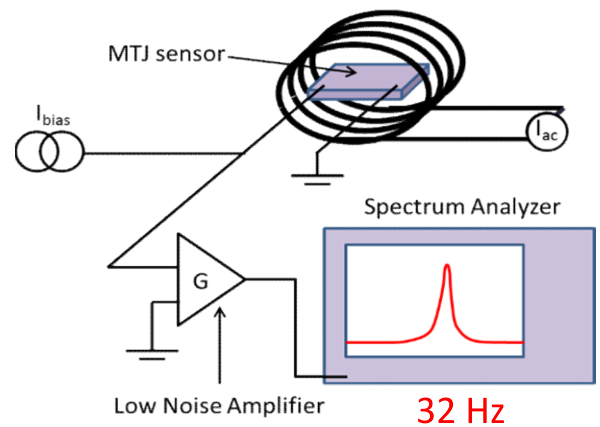

Detectivity limit:

SNR = 1
(Signal = Noise)

P.P.Freitas, R.Ferreira and S.Cardoso "Spintronic Sensors", **Proceedings of the IEEE**, 104, 1894 (2016)
E. Paz · S. Serrano-Guisan · R. Ferreira · P. P. Freitas – J. of Applied Physics; 115. 2014

Noise Spectrum of Magnetoresistive Sensors

Main noise contributions

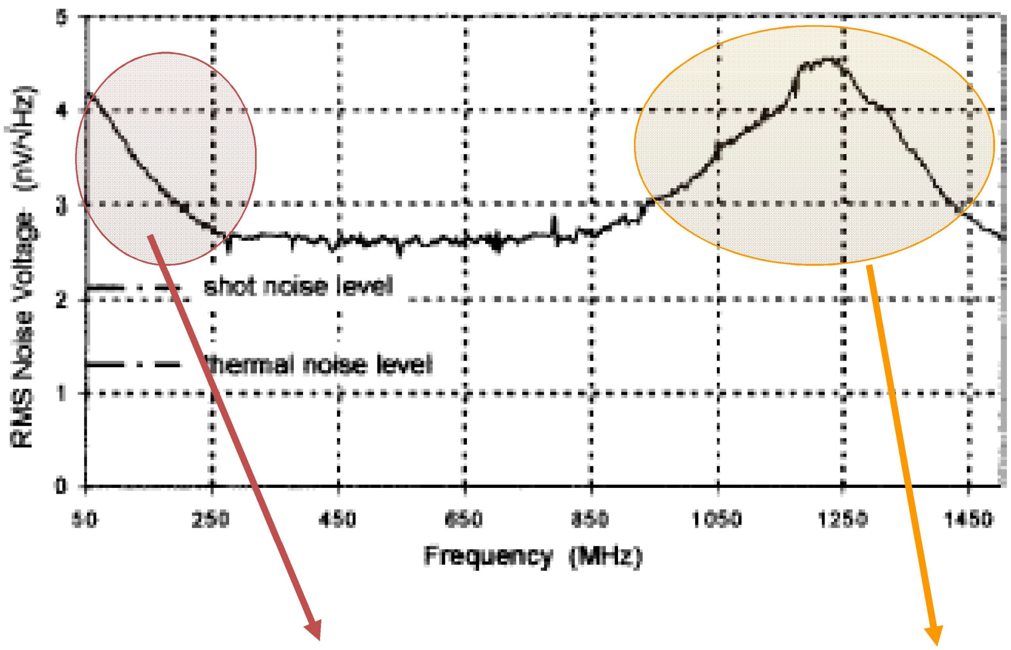

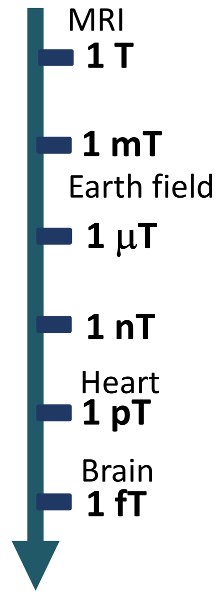

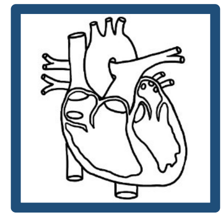

Amplitude:
few **pTesla** at chest surface
(below 100 Hz)

Amplitude:
few **fTesla** at skull surface
(below 100 Hz)

$$S_V(V^2/Hz) = \frac{\alpha_H I^2 R^2}{Af\ \Delta f} + \frac{4K_B TR}{\Delta f} + \frac{2eIR^2}{\Delta f} + FMR_{Noise}$$

1/f noise — Thermal Noise — Shot Noise — High-Frequency Noise

Field detectivity (D)

INESC MN
Microsistemas & Nanotecnologias

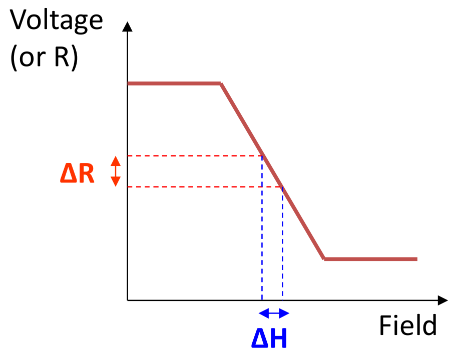

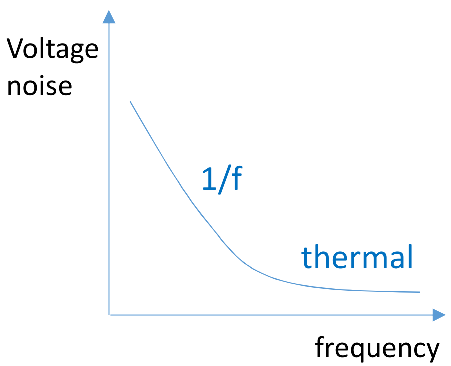

Detectivity limit: **SNR = 1** (Signal = Noise)

$$S_V\left(T/\sqrt{Hz}\right)=\frac{\sqrt{\dfrac{\alpha_H I^2 R^2}{V\ f}}}{I.\dfrac{\Delta R}{\Delta H}}=\frac{\Delta H}{MR}\sqrt{\frac{\alpha_H}{V\ f}}$$

[in Tesla]

(in 1/f regime)

Operate at high f
Increase MR
Increase V
Reduce linear range ΔH
Reduce Hooge value

S=TMR/ΔH
sensor sensitivity

α_H = Hooge's constant
A = MR area
f = operating frequency

INESC MN
Microsistemas & Nanotecnologias

Strategies to improve the minimum detectable field

Field modulation for high frequency

Increase MR

Increase V

Reduce linear range ΔH

Reduce Hooge value

Sensors, *18*(3), 790; (2018)

Micromachines, *7*(5), 88 (2016)

IEEE Trans. Magn. 48 (11), pp. 4115 (2012)

Journal of SPIN, Vol.1 (1), pp 71-91 (2011)

J.Appl.Phys. 103, 07E924 (2008)

Appl. Phys. Lett. 95, 023502 (2009)

magnetic MEMS

INESC MN
Microsistemas & Nanotecnologias

Modulate dc magnetic field at high frequency using MEMS resonators with incorporated magnetic flux guides

geometry

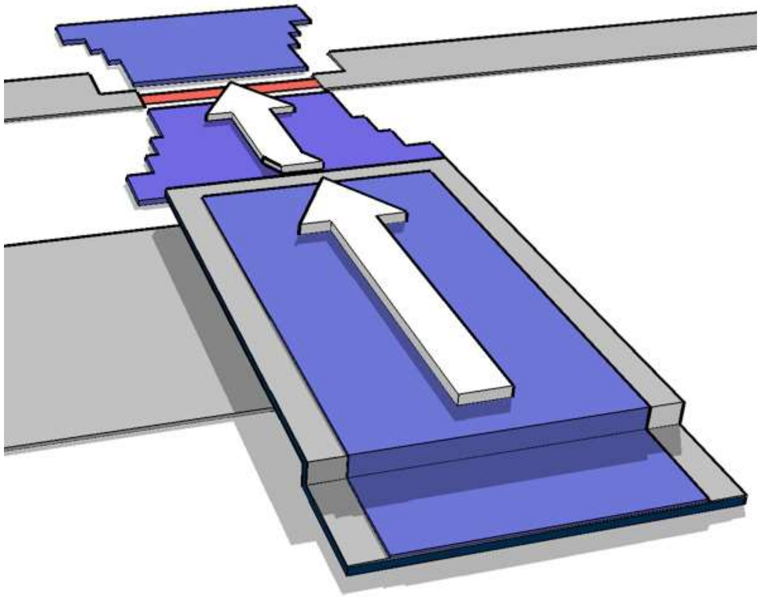

goal

shift the sensor operating frequency to the kHz region
where the noise can be 2 orders of magnitude lower then dc

spin valve noise spectrum

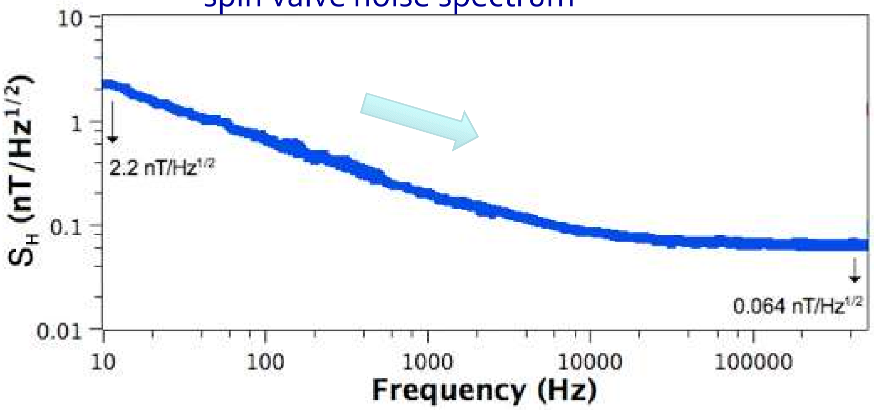

Appl. Phys. Lett. 95, 023502 (2009)

J.Appl.Phys. 103, 07E924 (2008)

Strategies to improve the minimum detectable field

Field modulation for high frequency

Increase MR

Increase A

Reduce linear range ΔH

Reduce Hooge value

Nat Mater, 2004, 3:862–867
J PhysD-Appl Phys, 2007, 40: R337
J. Physics: Cond.Matter, 19 (2007) 165221
Ann Rev Mater Res, 2009, 39: 277–296
J Appl Phys, 2007, 101: 09B501
J. Appl. Phys, 99, 08A907 2006

AlOx and MgO barriers

INESC MN
Microsistemas & Nanotecnologias

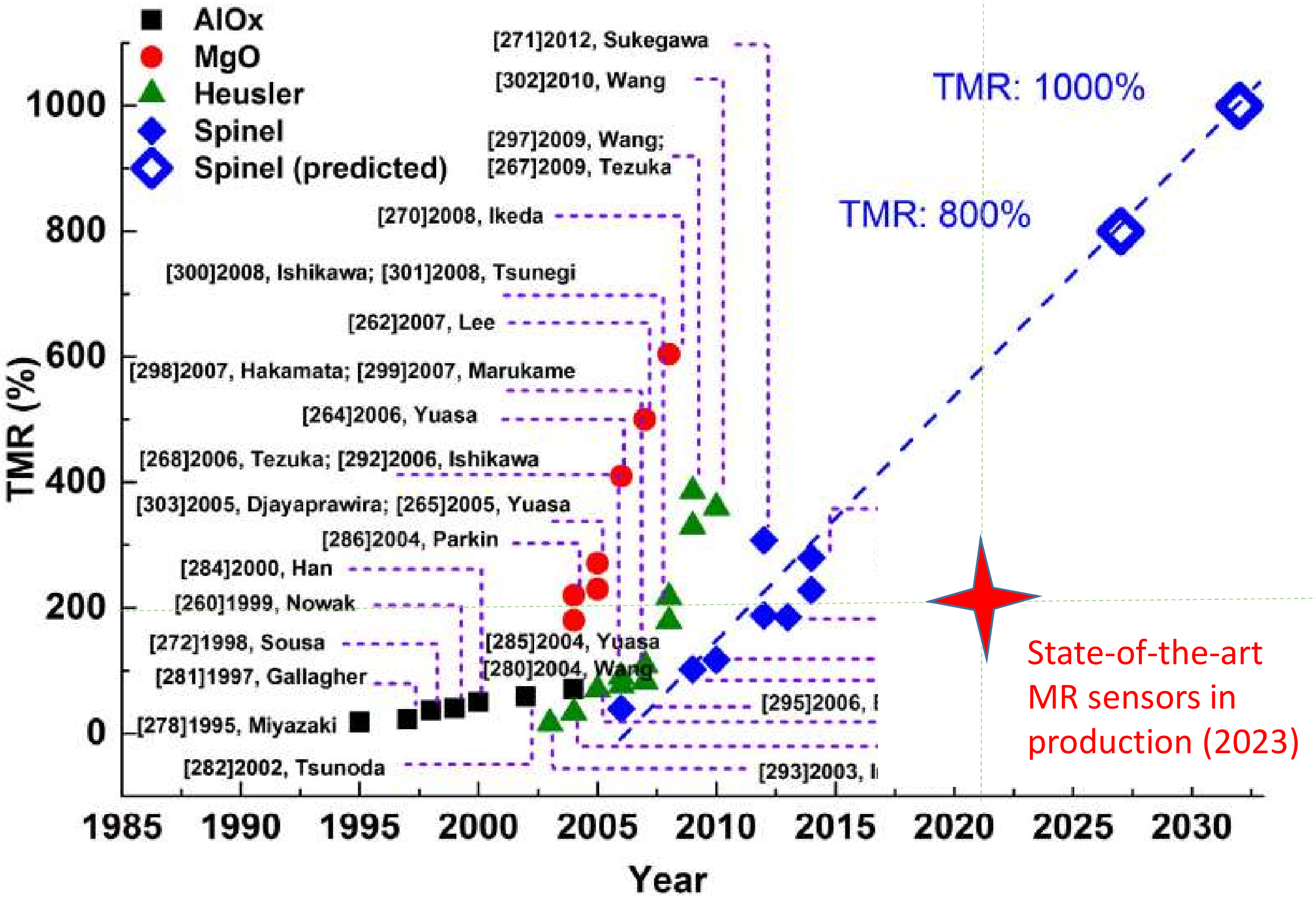

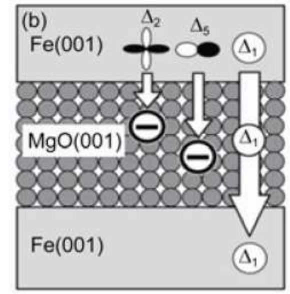

Crystalline barrier

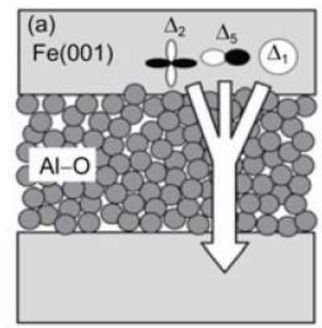

Amorphous barrier

"Magnetoresistive Sensor Development Roadmap (Non-Recording Applications)" IEEE Trans.Magn. (2019)

200mm backend GMR / TMR technology

INESC MN
Microsistemas & Nanotecnologias

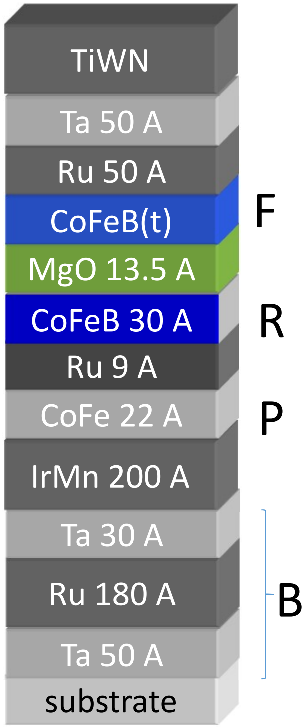

Nordiko
INNOVATION WITH RELIABILITY

6 targets IBD (extra module 8 targets in PVD; 2019)
Dep pressure 2 x 10^{-5}Torr
Heated substrate
Assist gun,
Base Pressure 5x10^{-8} Torr

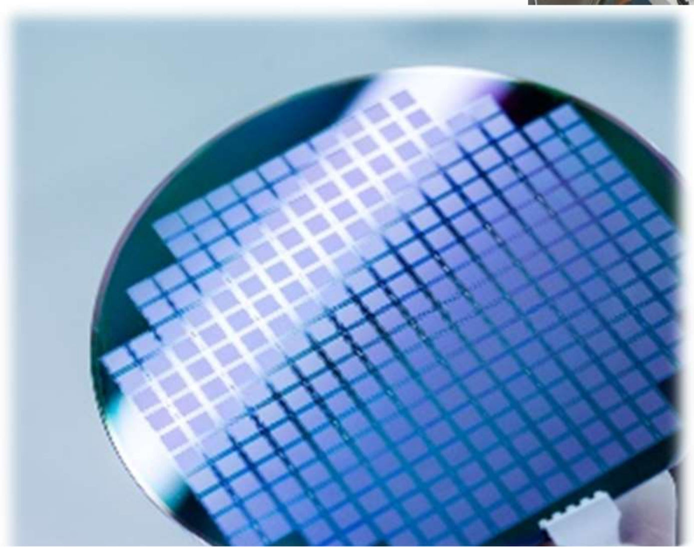

nffa.eu
ACEINNA
BOSCH
MagID
Inspectron
Track Trace Check Verify
LEMTECH
MASMA
SME Instrument
TUMAPOS
SME Instrument
Allegro MicroSystems, LLC
High-Performance Semiconductors
BOGEN

MgO TMR sensors

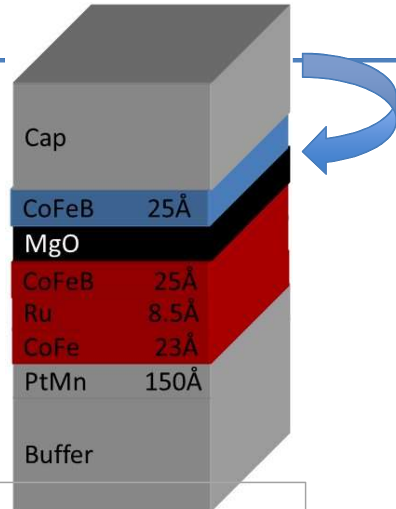

Amorphous CoFeBSi , CoFeBTa

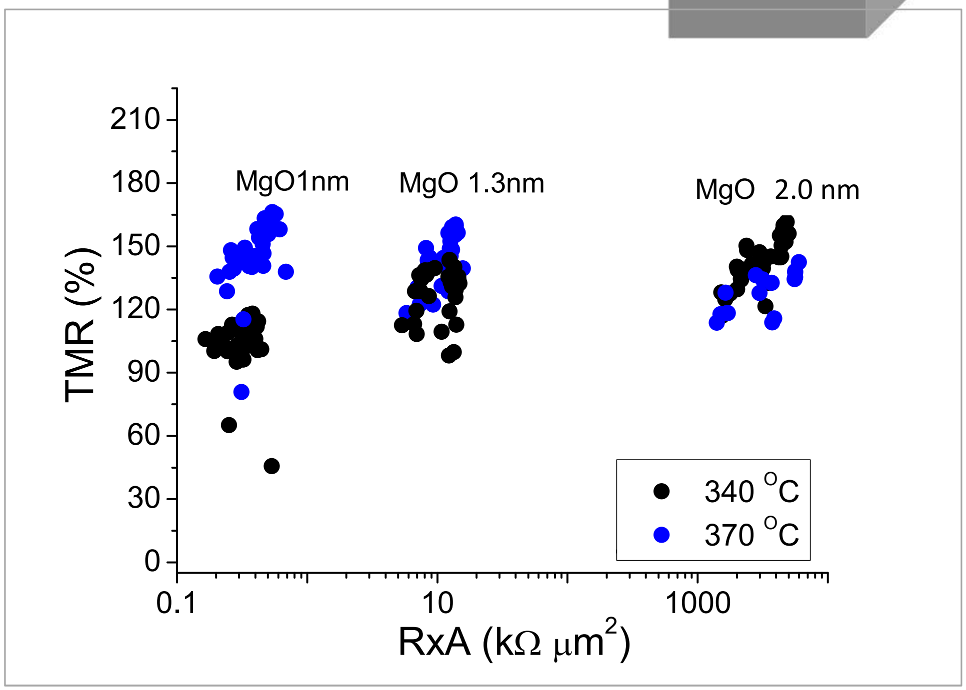

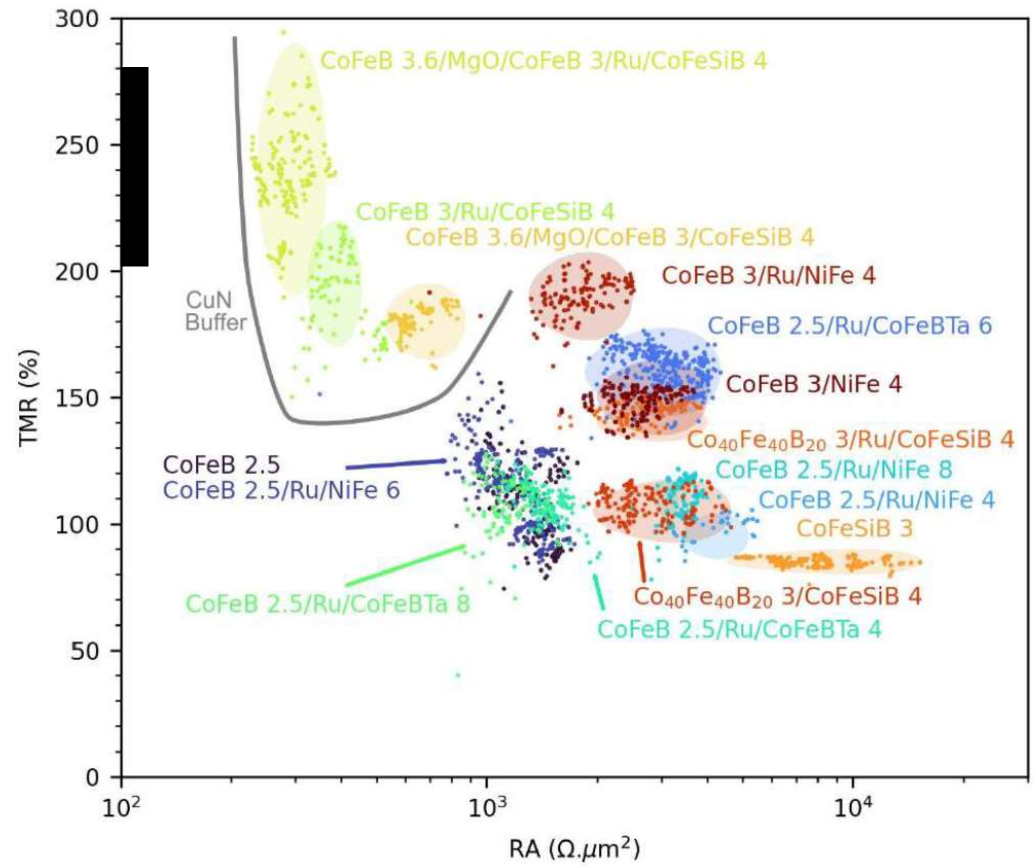

F.Matos, et.al. **AIP-Advances**, 13, 025108 (2023);

Strategies to improve the minimum detectable field

- Field modulation for high frequency
- Increase TMR
- **Increase V (area or thickness)**
- Reduce linear range ΔH
- Reduce Hooge value

R.Chaves, et.al , Appl. Phys.Lett, 91, 102504 (2017)
E. Paz et.al – J. Applied Physics; 115. 2014

INESC MN
Microsistemas & Nanotecnologias

Large Series
1102 TMR elements with
A= 100x100 μm² each.

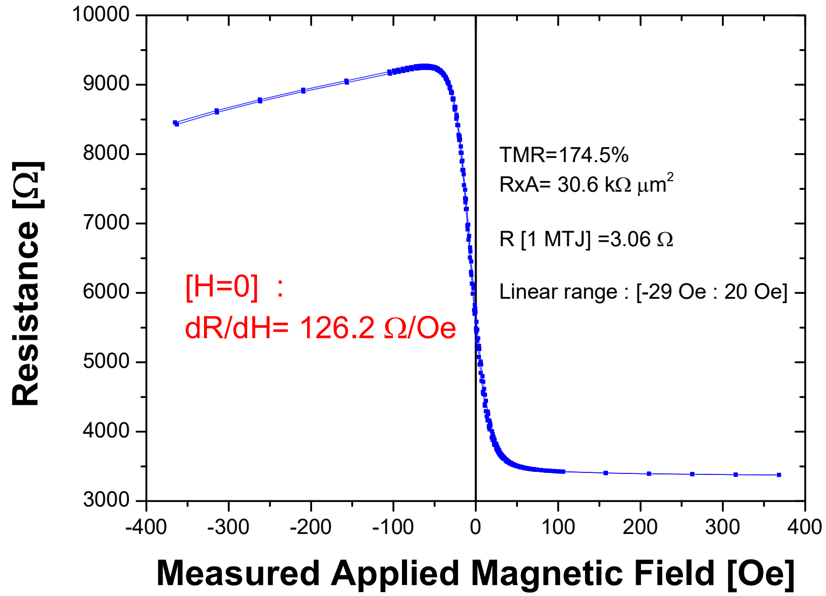

INL INTERNATIONAL IBERIAN NANOTECHNOLOGY LABORATORY

1 mm x 1 mm

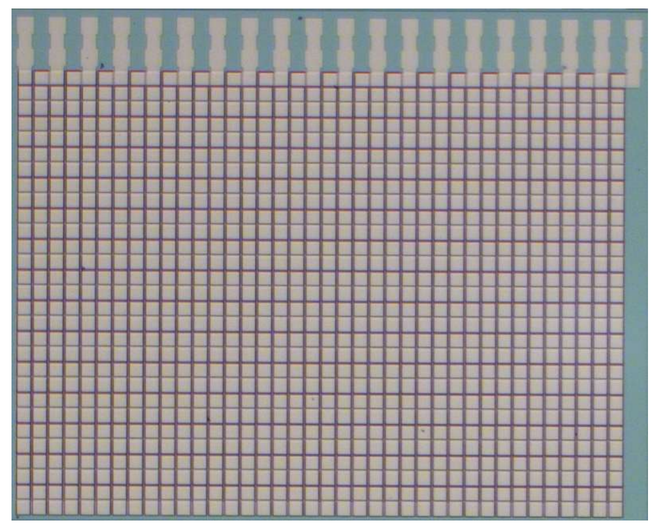

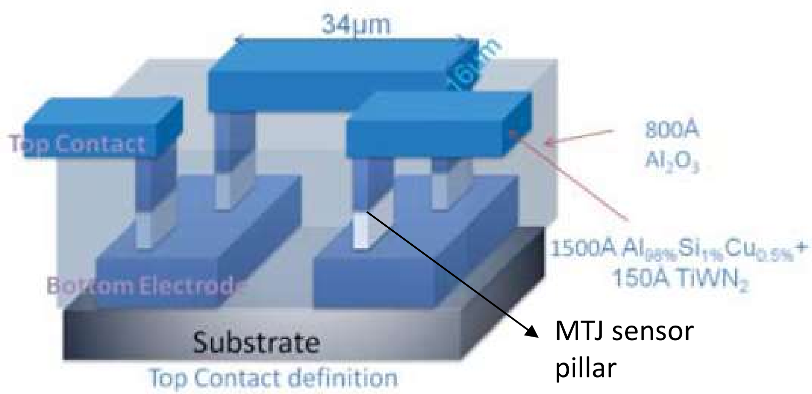

E. Paz · S. Serrano-Guisan · R. Ferreira · P. P. Freitas - Journal of Applied Physics; 115. 2014

Saving space: GMR sensors packed

INESC MN
Microsistemas & Nanotecnologias

Single sensor

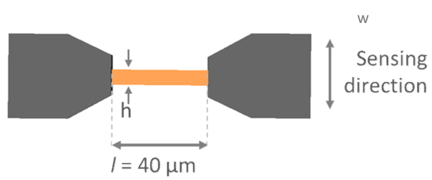

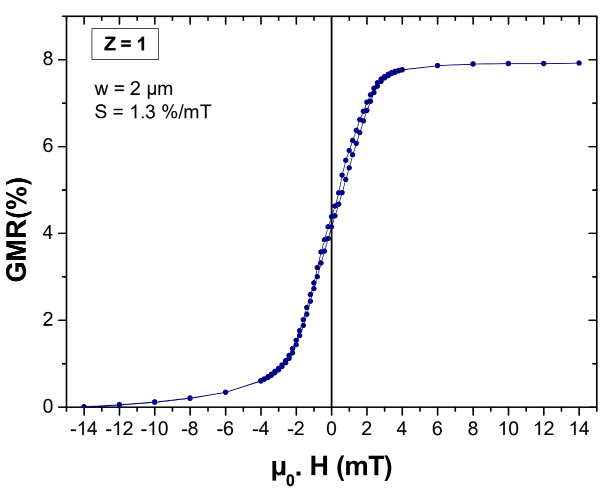

Packed sensors

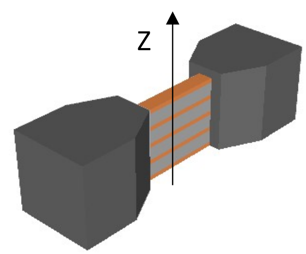

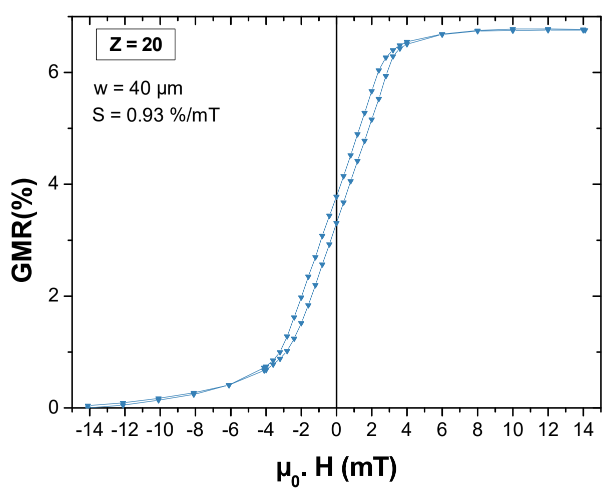

Packed arrays of sensors

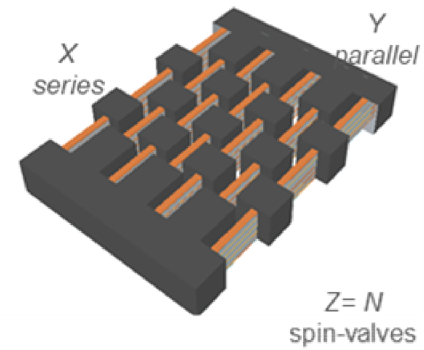

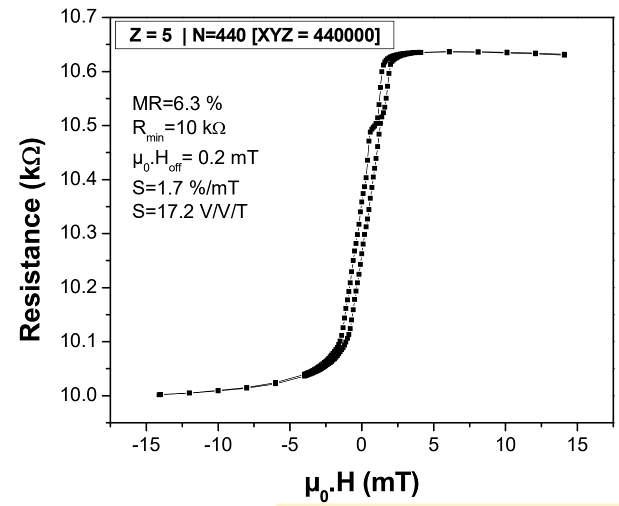

AIP Advances 8(5):056644 (2018)
Scientific Reports , 11, 215 (2021)

INESC MN
Microsistemas & Nanotecnologias

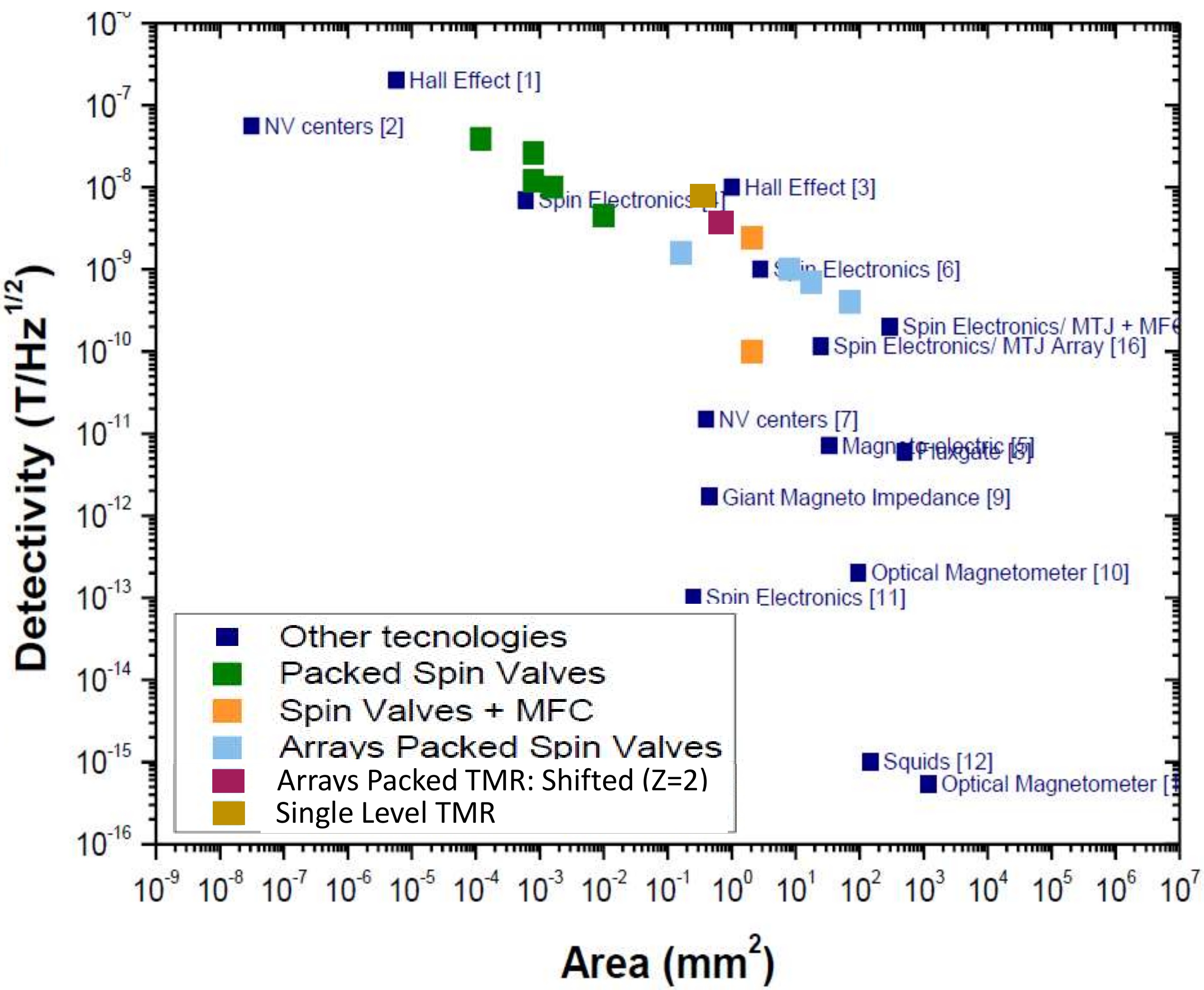

AIP Advances 8(5):056644 (2018)
Scientific Reports , 11, 215 (2021)

[1] E. Paz et al., *J. Appl. Phys.*, vol. 115,2014.
[2] tdk.com, "TDK biomagnetic sensor", 2019
[3] S. H. Liou *et al.*, *Proc. IEEE Sensors*, 2009

[1] P. Besse *et al* Appl. Phys. Lett. **80**, 4199 (2002)
[2] P. Maletinsky et al Nature Nanotechnology 7, 320-324 (2012)
[3] F. Montaigne et al Sensors and Actuators A: Physical 81, 324-327 (2000)
[4] L. Caruso et al Neuron 95, 1283-1291 (2017)
[5] R. Jahns et al Sensors and Actuators A: Physical 183, 16-21 (2012)
[6] F. Barbieri et al Scientific Reports 6, 39330 (2016)
[7] J. Barry et al PNAS 113, 14133-14138 (2016)
[8] Bartington Instruments, Mag-03 Three-axis
[9] S. Yabukami et al JMMM 290, 1318-1321 (2005)
[10] T. Sander et al Biomedical Optics Express 3, 981-990 (2012)
[11] M. Pannetier et al Science 304, 1648-1650 (2004)
[12] J. Gallop Supercond. Sci. Technol. 16, 1575 (2003)
[13] I. Kominis et al Nature 422, 596-599 (2003)
[14] E. Paz et al., *J. Appl. Phys.*, vol. 115,2014.
[15] tdk.com, "TDK biomagnetic sensor", 2019
[16] S. H. Liou *et al.*, *Proc. IEEE Sensors*, 2009

Applications

- Neurosciences
- Robotics
- Pattern readout
- Biochips

If no time: move to end

INESC MN
Microsistemas &
Nanotecnologias

Applications

Neuronal probes with MR sensors

INESC MN
Microsistemas & Nanotecnologias

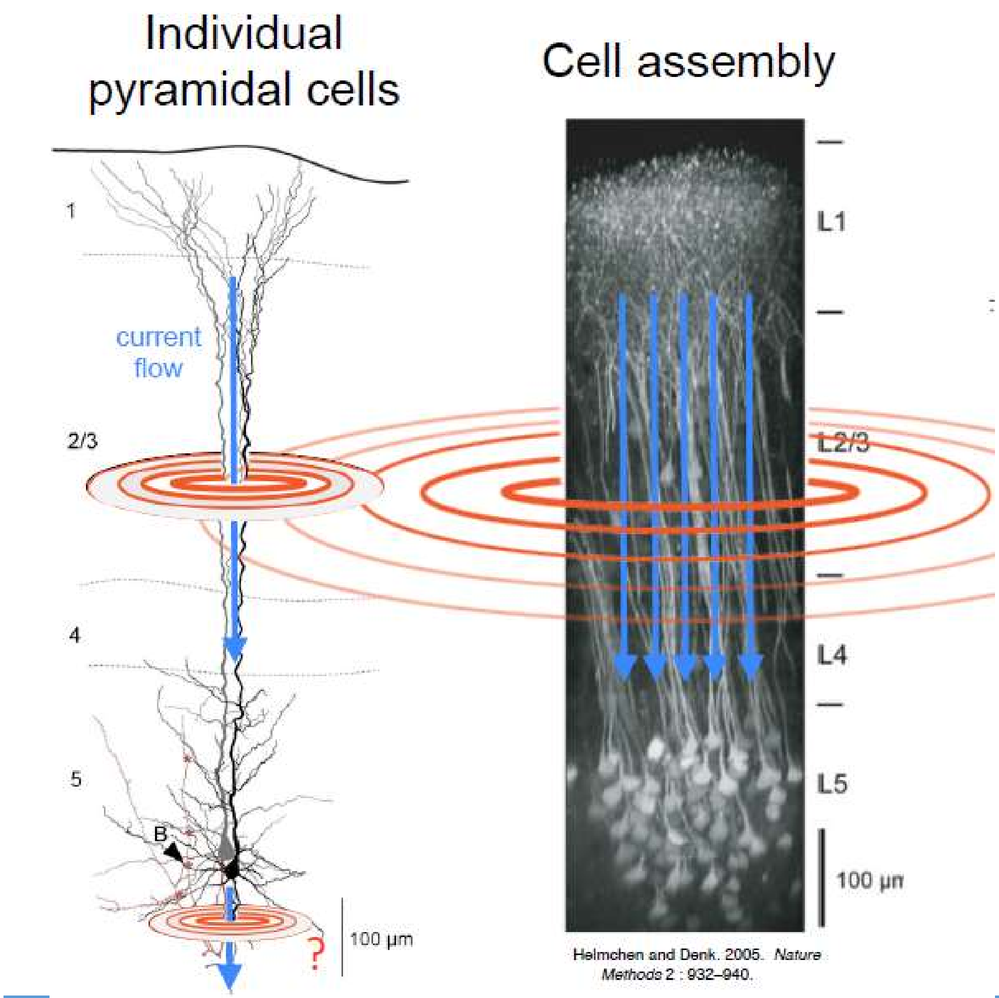

Estimation of the magnetic field:

- **MagnetoEncephaloGraphy :**
  SQUID - signal distance = 3 cm
  Field = 1 fT (Field decay : $1/(r^2)$)
- **Magnetrodes:**
  MR - signal distance = 10-100 µm
  Field ≈ 100 pT – 1nT

Estimated fields ~pT - nT

FET-EU project Magnetrodes

INESC MN
Microsistemas & Nanotecnologias

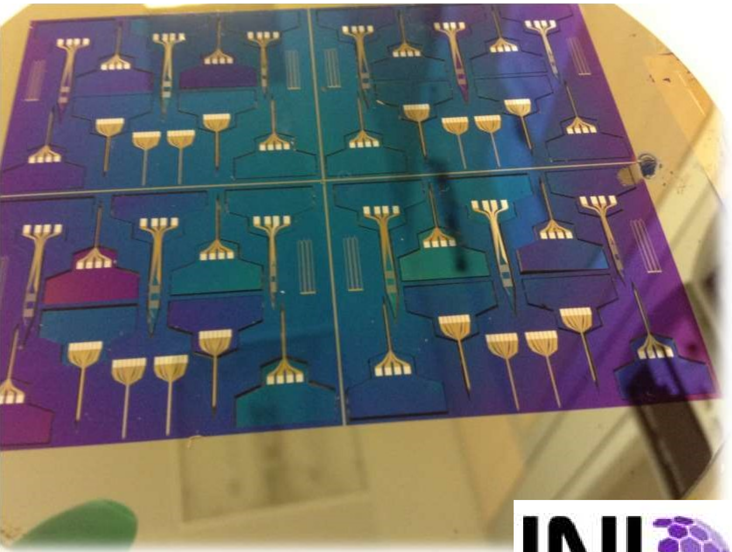

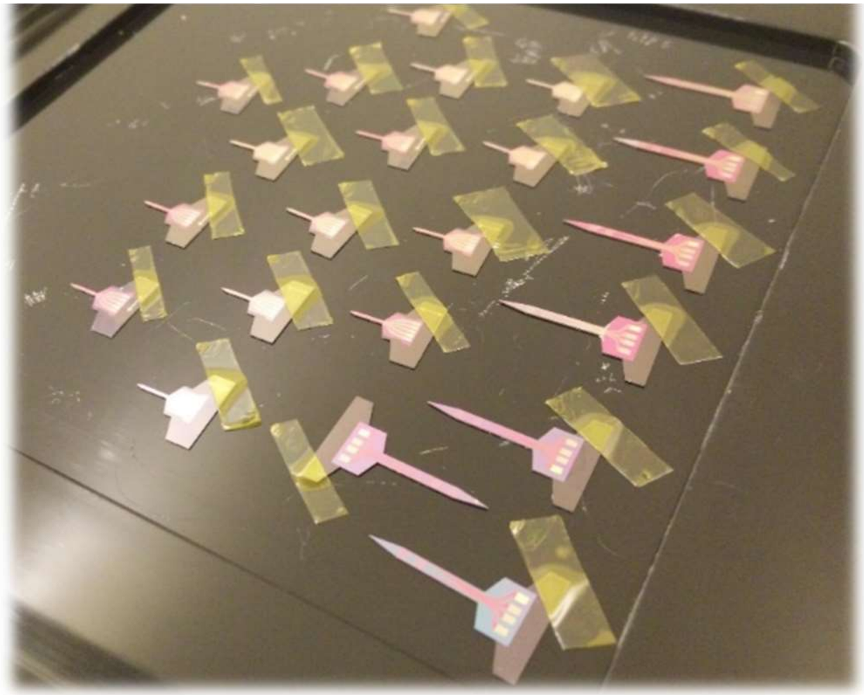

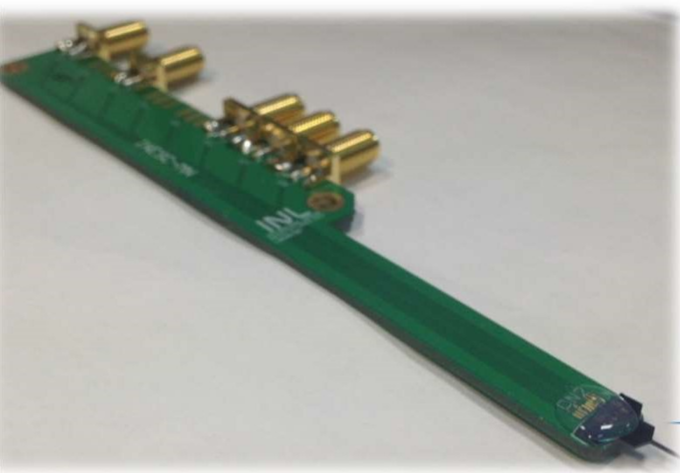

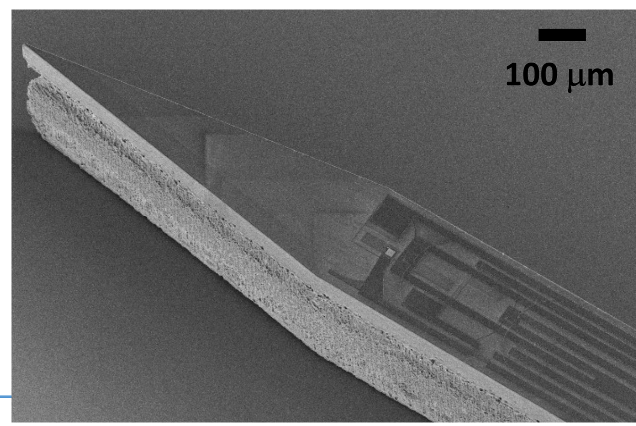

SEM image: sharp tip (*in-vivo*)

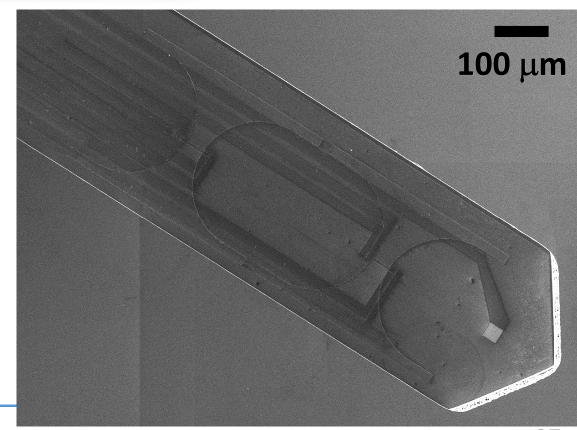

SEM image: flat tip (*in-vitro*)

When penetrating the tissues:

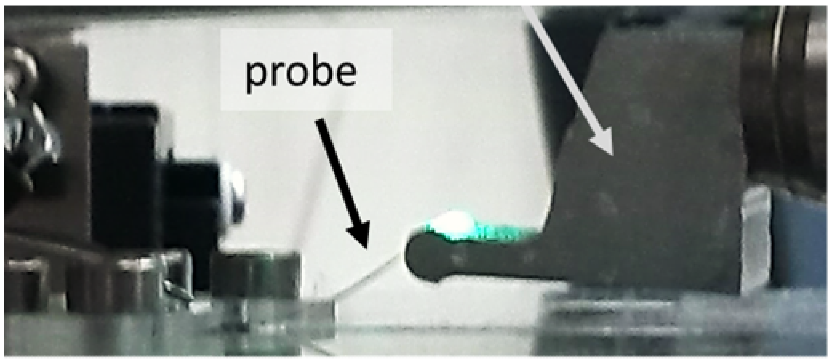

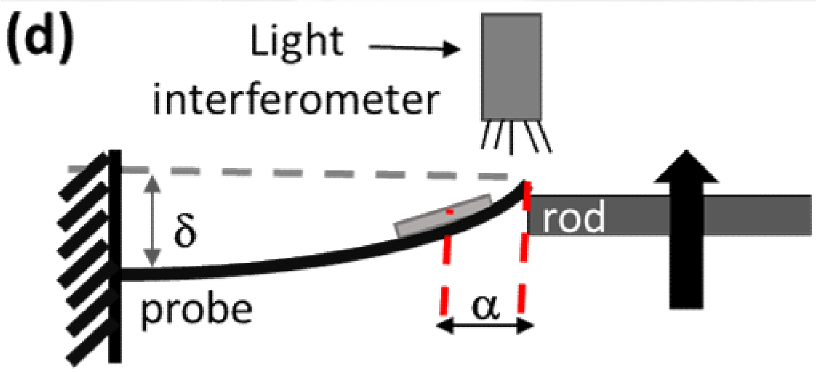

- axial force along the tip longitudinal direction;
- slight bending of the probe, **force perpendicular to the longest direction.**

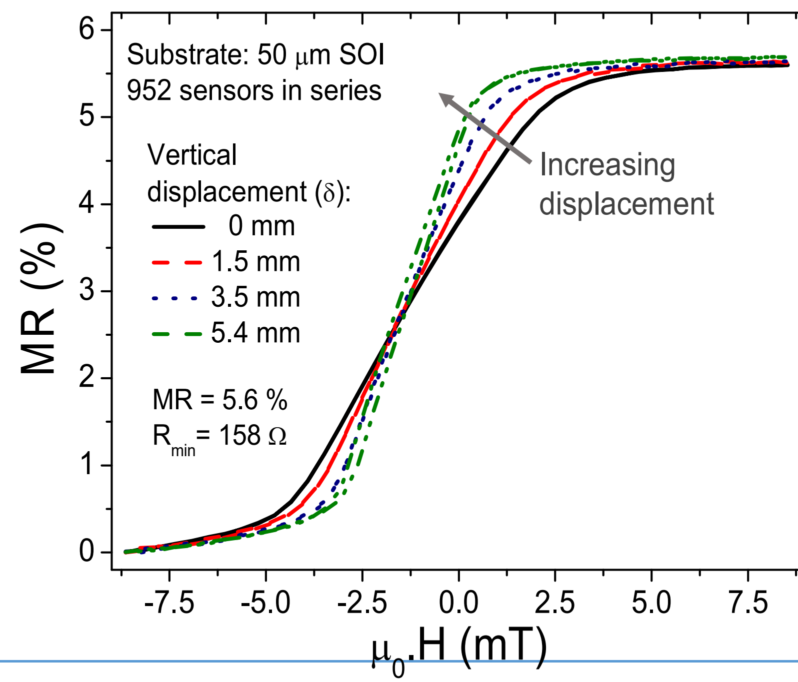

Sensor output: remains linear, non-hysteretic and without discontinuities

Valadeiro et al IEEE Trans Mag 51 (2015) 4401104

In Vivo validation of MR sensor probes

INESC MN
Microsistemas & Nanotecnologias

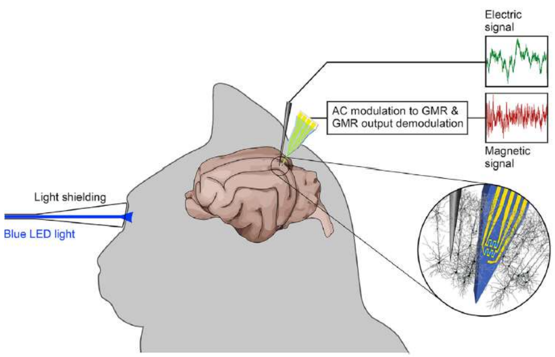

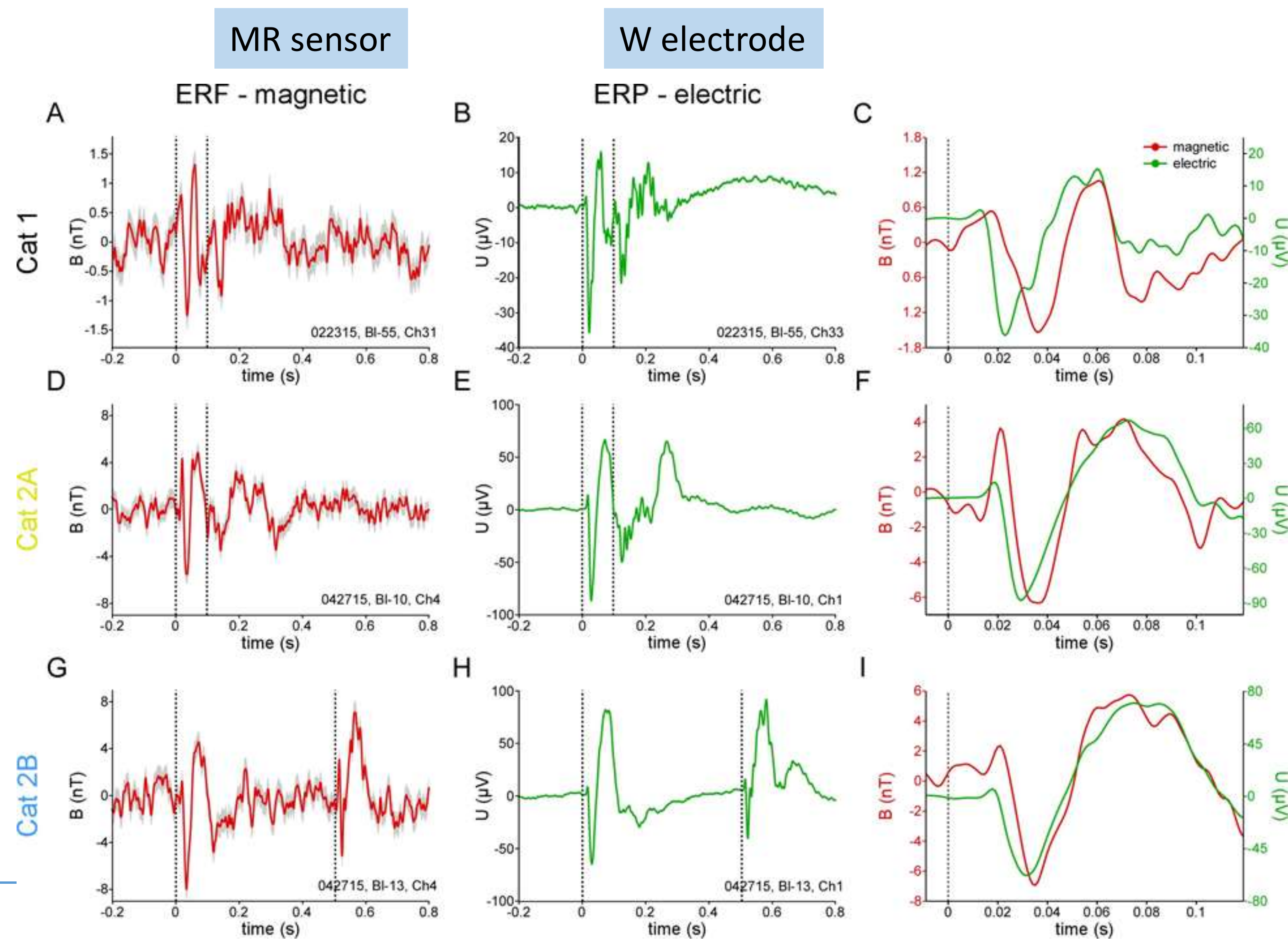

L.Caruso, S.Cardoso, P.P Freitas, P.Fries, M. Lecoeur, et.al
"In vivo magnetic recording of neuronal activity",
***Neuron,** 95, 1–9 (2017)*

INESC MN
Microsistemas & Nanotecnologias

Detectivity (D) - **minimum detectable field**
SNR =1

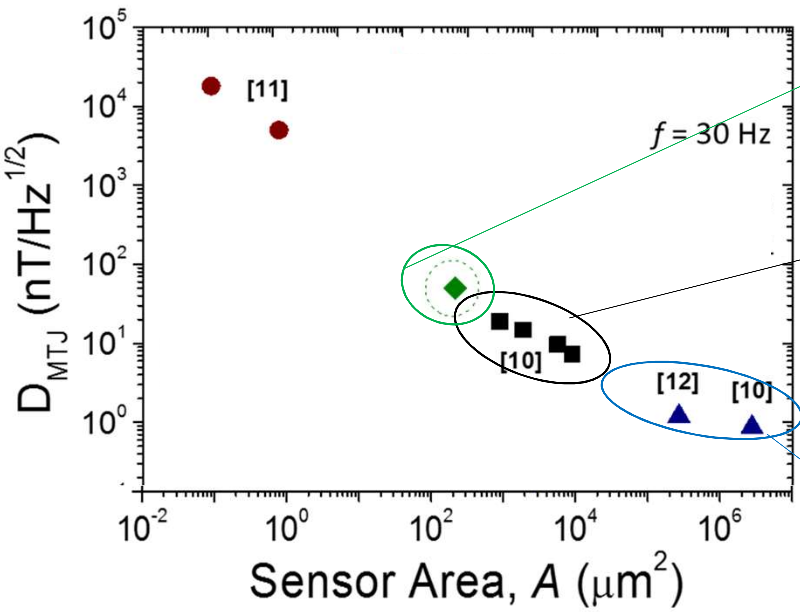

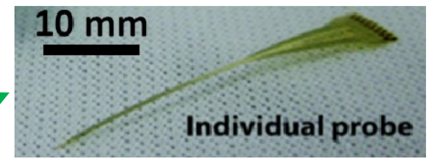

flexible probe - polyimide

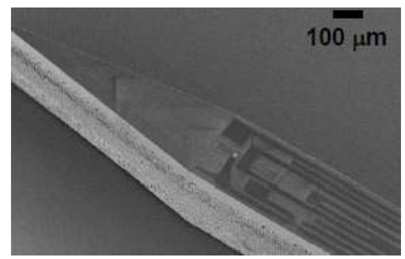

Si probe (single MR)

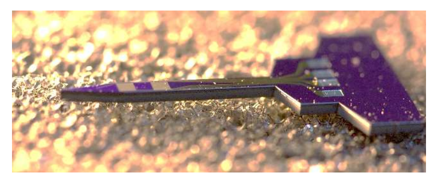

Si probe (arrays MR)

IEEE Trans Magn. vol. 51 (11) 4401104 (2015)
J.Gaspar et.al, IEEE Trans Magn. Vol.53 (4), 5300204 (2017

Applications in robotics

INESC MN
Microsistemas & Nanotecnologias

The Vizzy hand

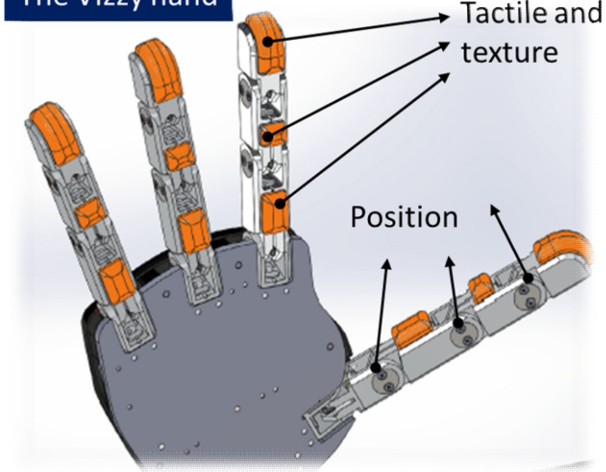

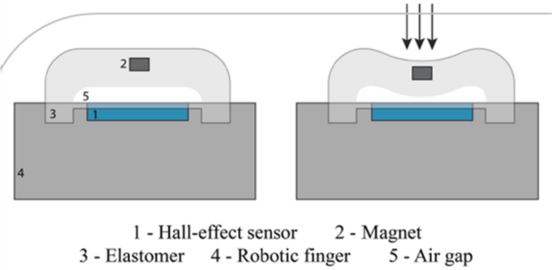

3D Hall effect pressure sensors

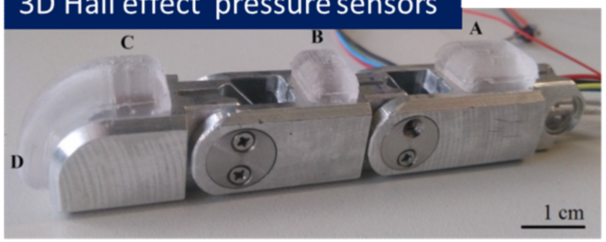

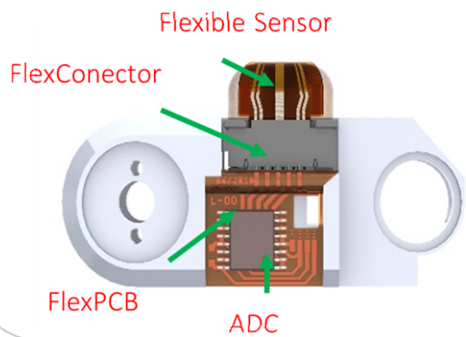

Flexible 2D GMR pressure sensors

Distributed GMR/TMR sensors

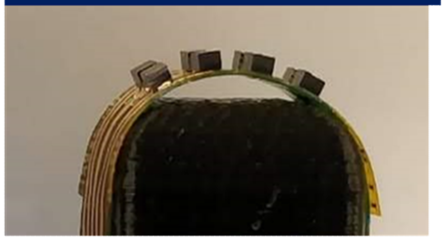

2D MR sensors mounted by flip-chip

Cilia + 2D GMR tactile and pressure sensors

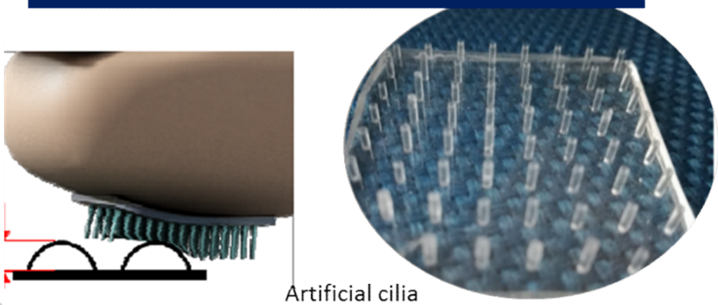

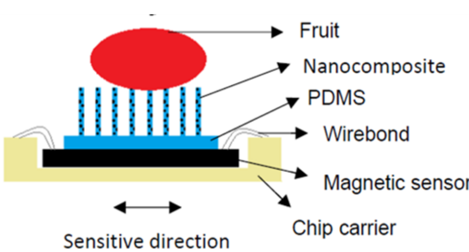

If no time:move to

Institute for Systems and Robotics Lisboa · CRISP · Advanced Robotics @ Queen Mary ARQ · INESC MN Microsistemas & Nanotecnologias

Magnetic cilia bending **induces** magnetic profile variation

MR sensor transduces variation into an electrical signal

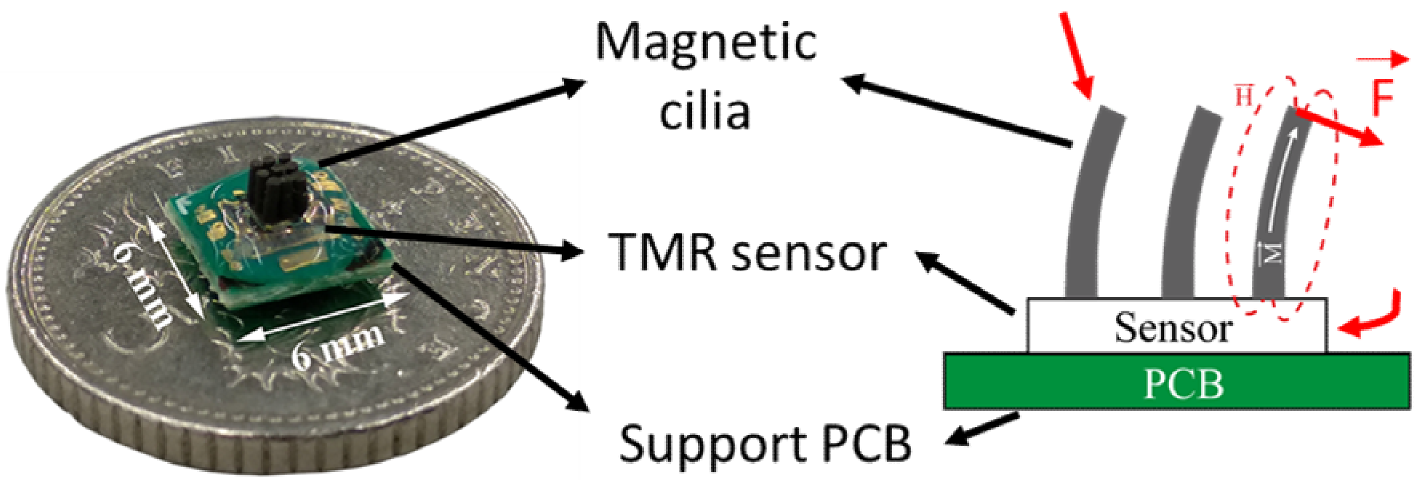

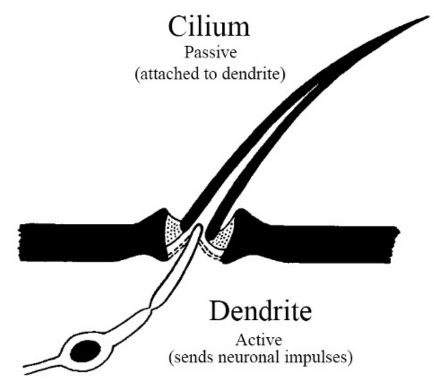

A. Alfadhel and J. Kosel, Advanced Materials, 27, 7888–7892, 2015.
P. Ribeiro, et.al. IEEE Robotics and Automation Letters, 2, 971–976, 2017.

Institute for Systems and Robotics Lisboa | CRISP | Advanced Robotics @ Queen Mary ARQ | INESC MN Microsistemas & Nanotecnologias

Mechanical simulation (FEM – with COMSOL)

Magnetic moment simulation

Magnetic moment simulation

Deformation

Magnetic field

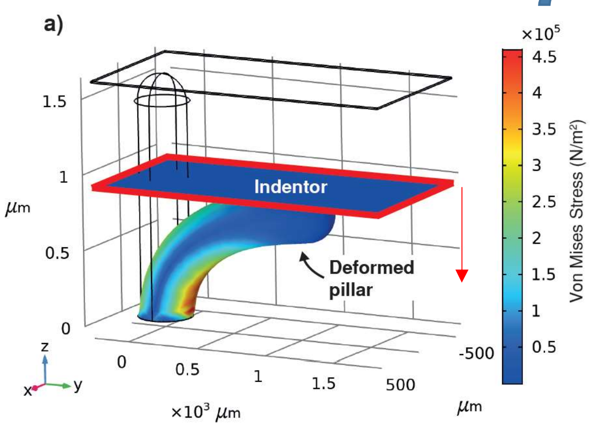

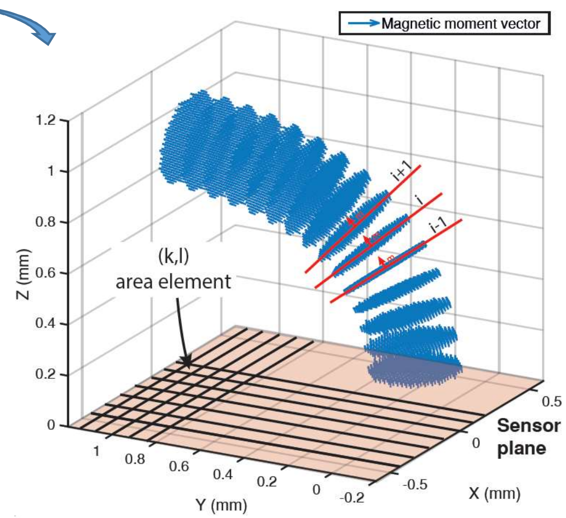

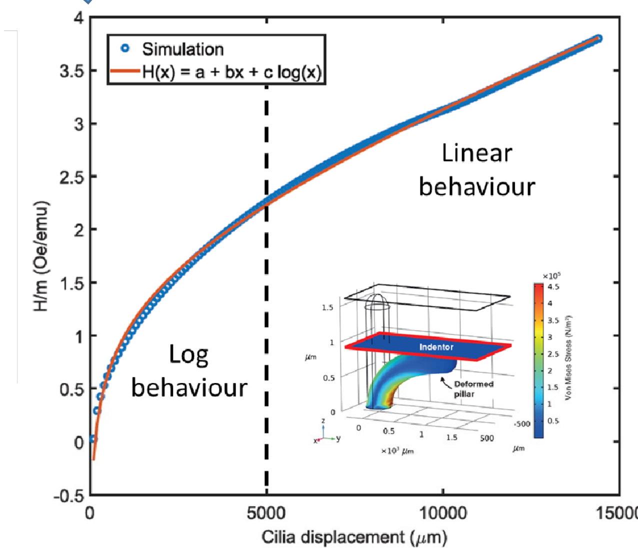

Simulation: indentor iteratively lowered against cilia
Steps of 100 µm
Discretized into cross-sections

$$\mathbf{v}_{i-1} = \overrightarrow{i-1, i}; \ \mathbf{v}_{i+1} = \overrightarrow{i, i+1}$$
$$\mathbf{v}_i = \frac{\mathbf{v}_{i+1} + \mathbf{v}_{i-1}}{2}.$$

Estimation of **m** direction

$$\mathbf{H}_j(r_{j,(k,l)}) = \frac{1}{4\pi}\left(\frac{3\mathbf{r}_{j,(k,l)}(\mathbf{m}_j \cdot \mathbf{r}_{j,(k,l)})}{|\mathbf{r}_{j,(k,l)}|^5} - \frac{\mathbf{m}_j}{|\mathbf{r}_{j,(k,l)}|^3}\right)$$

H (x direction) over surface

$$\langle \mathbf{H}_{inc} \rangle = \frac{\sum_{k=1}^{N_k}\sum_{l=1}^{N_l}\sum_{j=1}^{N} \mathbf{H}_j(r_{j,(k,l)})}{N_k N_l}$$

Average field over sensor area

$$\langle H \rangle(x) = ax + b\log(x) + c$$

Best fitting function describing field

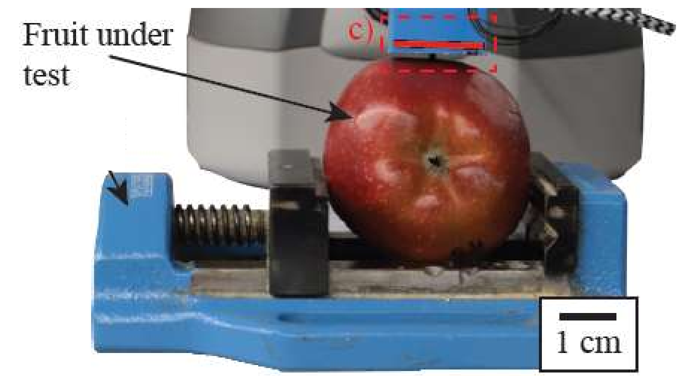
Fruit under test
c)
1 cm

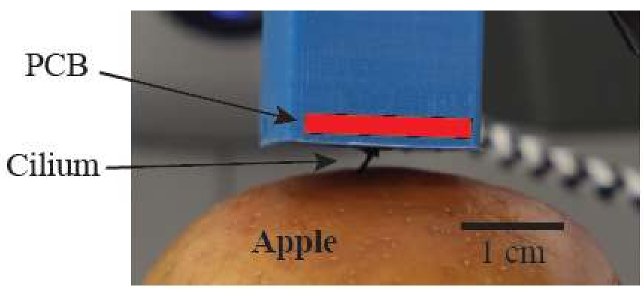
PCB
Cilium
Apple
1 cm

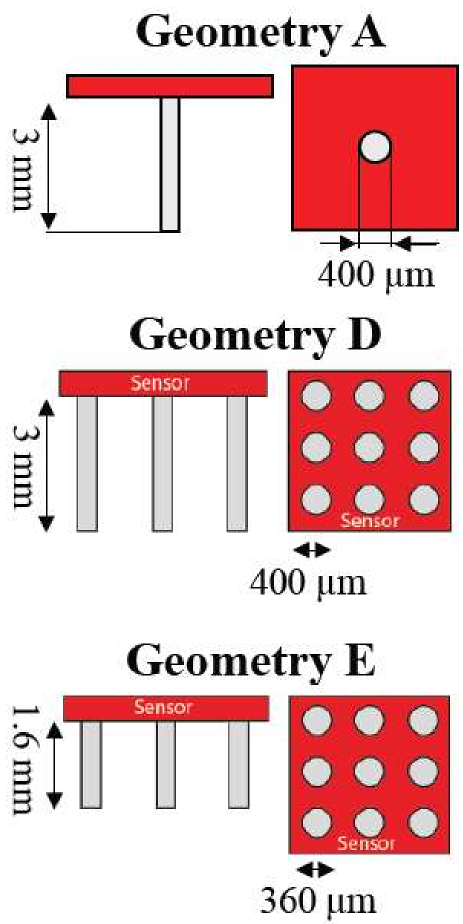
Geometry A
3 mm
400 µm
Geometry D
Sensor
3 mm
Sensor
400 µm
Geometry E
Sensor
1.6 mm
Sensor
360 µm

Institute for Systems and Robotics Lisboa | CRISP | Advanced Robotics @ Queen Mary ARQ | INESC MN Microsistemas & Nanotecnologias

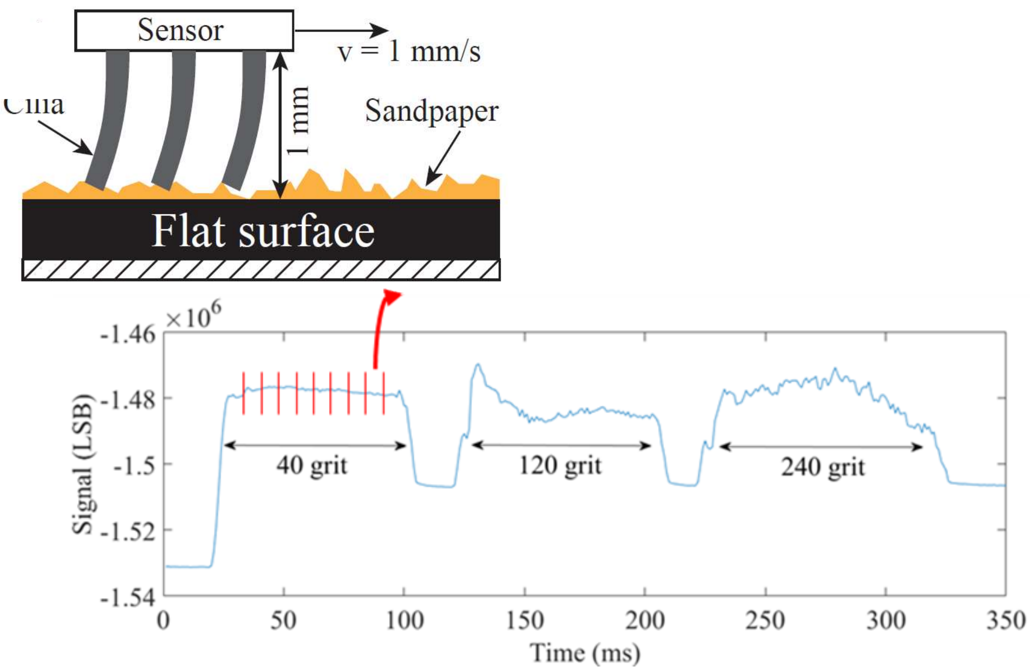

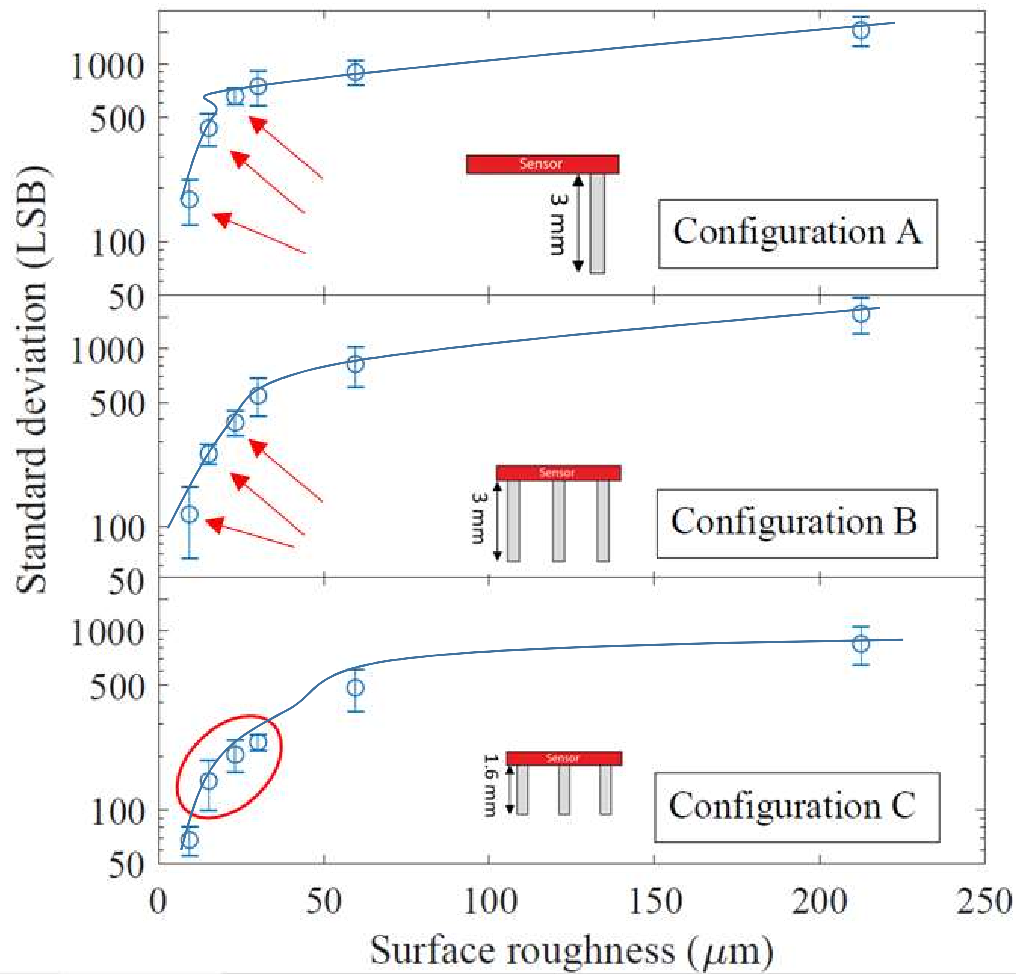

- Surface roughness from the signal standard deviation
- **Configuration A and B provide better resolution**
- 5.9 µm resolution

P.Ribeiro et.al., ICRA 2019

P.Ribeiro et.al., IROS 2020 : International Conference on Intelligent Robots and Systems 2020

 

Proof of concept
Fruit quality classifier

Braeburn apples
- 12 ripe fruits
- 12 senescent fruits

Sabrina strawberries
- 12 ripe fruits
- 12 senescent fruits

Data acquisition
- Data rate: 1 kSPS
- Scan speed: 1 mm/s
- 10 consecutive scans in each area
- 2 areas per fruit

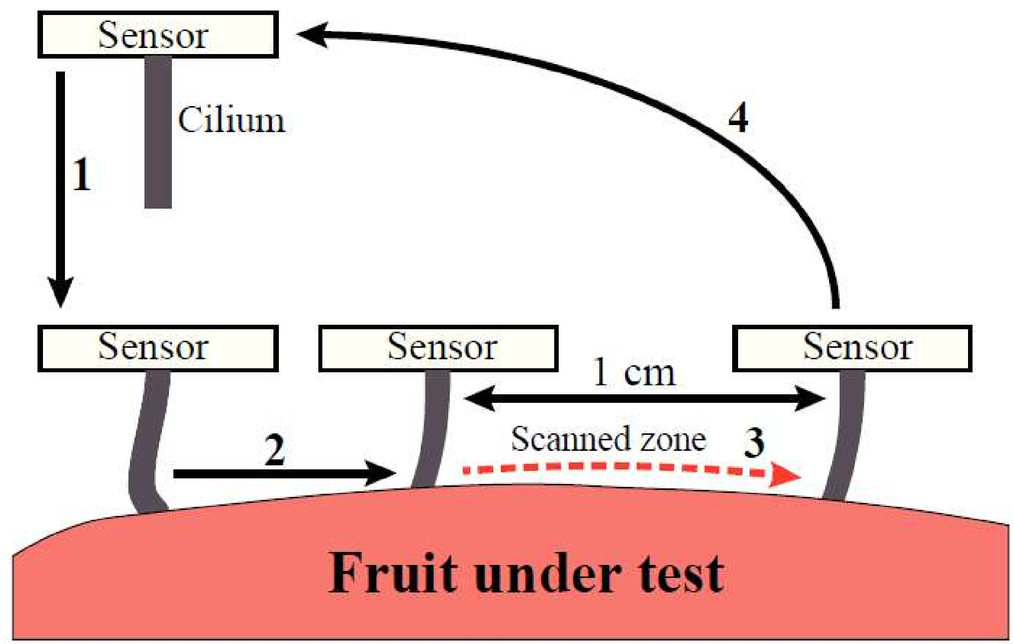

FRUIT QUALITY SENSING - RESULTS

TÉCNICO LISBOA | Institute for Systems and Robotics Lisboa | CRISP | Advanced Robotics @ Queen Mary ARQ | INESC MN Microsistemas e Nanotecnologias

Raw signal upon scanning

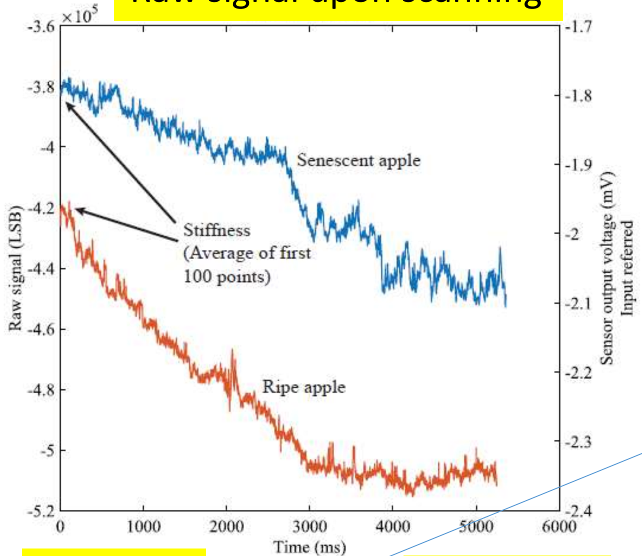

Waviness

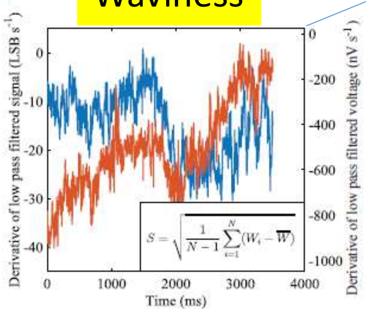

Roughness

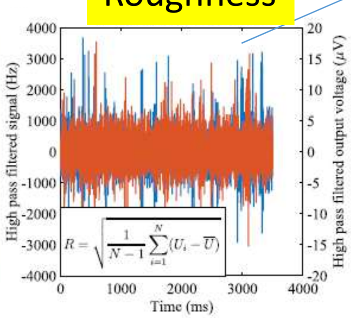

3 features were extracted from the signal

FEATURE	WHAT IS MEASURED	PHYSICAL CHARACTERISTIC
Stiffness (E)	Sensor signal with achieved contact	Fruit hardness
Waviness (S)	Std. deviation of 100 point moving average	Deformation over fruit surface
Roughness (R)	Std. deviation of high-pass filtered (f > 150 Hz) signal	Fruit surface texture

Fruit can be classified into two classes → **Ripe** / **Senescent**

FRUIT QUALITY SENSING - RESULTS

Stiffness (E) → Fruit hardness

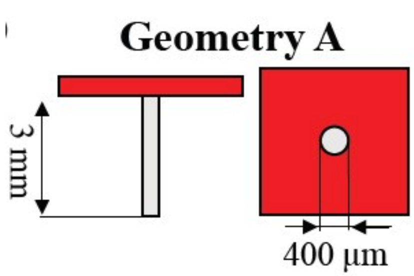

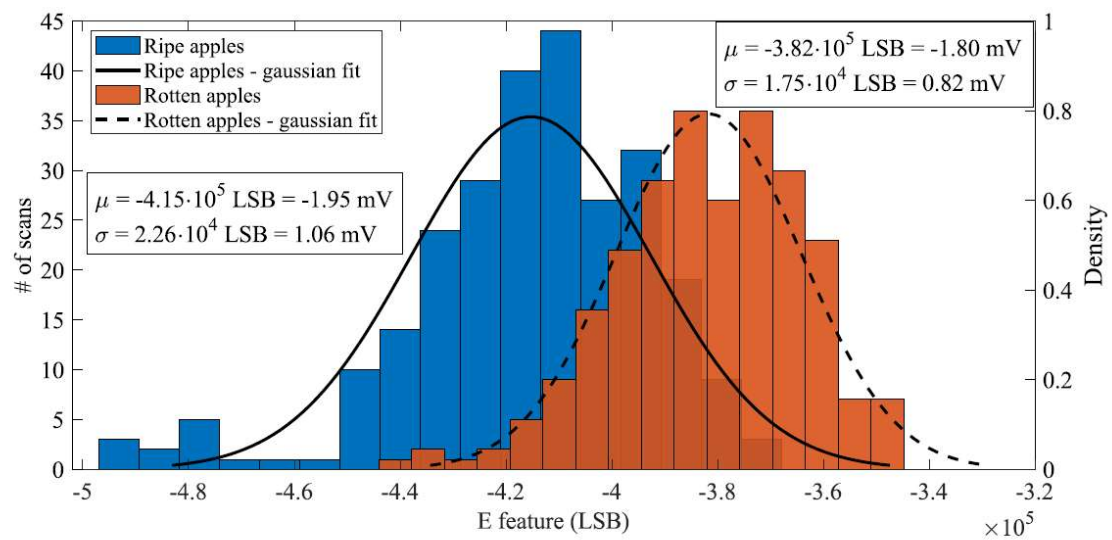

Figure 6.4: Computed E parameter histogram from all scans of apples scanned using a geometry A ciliary sensor.

Gaussian classifier

(Gaussian Näive Bayes)

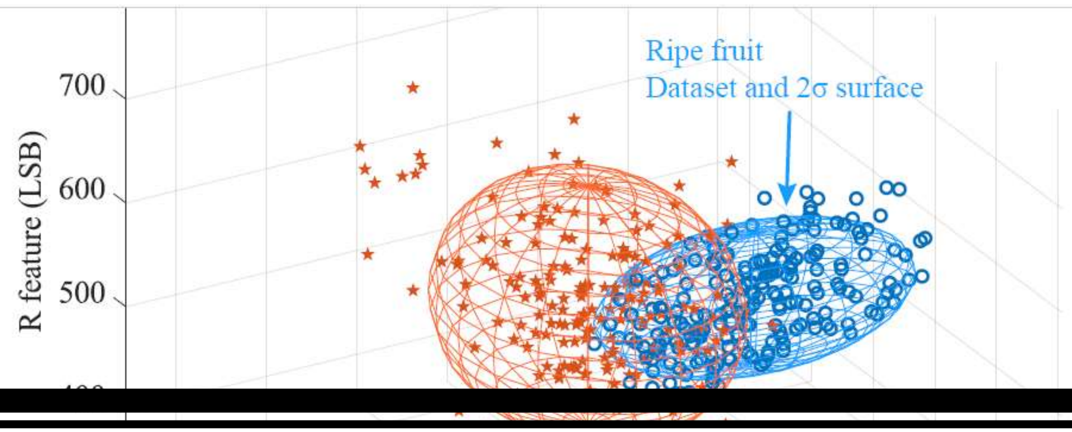

Combining

R, S, E

Sensor	Fruit	1 feature (E)	2 features ($E+R$)	3 features ($S+E+R$)
B	Apple	0.83	0.92	0.96
	Strawberry	0.63	0.79	0.71
D	Apple	0.71	0.88	0.88
	Strawberry	0.67	0.67	0.71
E	Apple	0.58	0.71	0.71
	Strawberry	0.63	0.83	0.83

Table 6.3: Accuracy vs number of features used for classification with Gaussian Näive Bayes algorithm.

FRUIT QUALITY SENSING - RESULTS

Apple

Strawberry

Conf. A

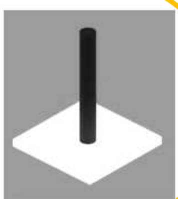

h = 3 mm
ϕ = 400 µm

Apple:

	True positive	True negative	Accuracy
Naïve Bayes	11/12	12/12	0.96
Random Forest	10/12	12/12	0.92

Strawberry:

	True positive	True negative	Accuracy
Naïve Bayes	7/12	10/12	0.71
Random Forest	8/12	11/12	0.79

Conf. B

h = 1.6 mm
ϕ = 320 µm

Apple:

	True positive	True negative	Accuracy
Naïve Bayes	10/12	11/12	0.88
Random Forest	10/12	11/12	0.88

Strawberry:

	True positive	True negative	Accuracy
Naïve Bayes	10/12	7/12	0.71
Random Forest	10/12	10/12	0.83

Conf. C

h = 3 mm
ϕ = 400 µm

Apple:

	True positive	True negative	Accuracy
Naïve Bayes	9/12	8/12	0.71
Random Forest	9/12	11/12	0.83

Strawberry:

	True positive	True negative	Accuracy
Naïve Bayes	10/12	10/12	0.83
Random Forest	10/12	10/12	0.83

“From farm to fork”

INESC MN
Microsistemas & Nanotecnologias

Final food inspection

Integrated Food control & management system

If no time: move to

Magnetic Biosensors and biomedical interfaces

INESC MN
Microsistemas & Nanotecnologias

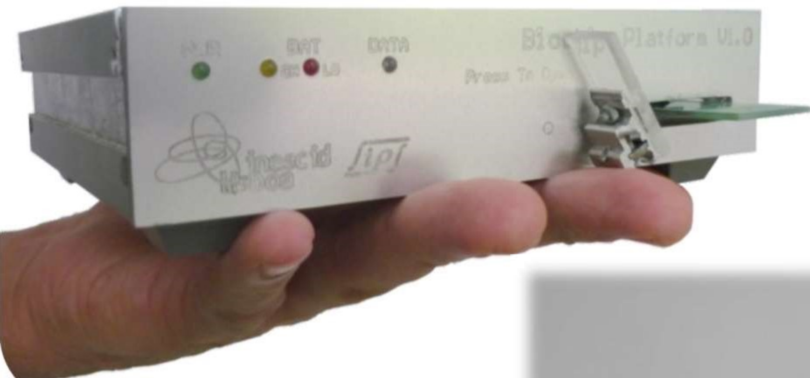

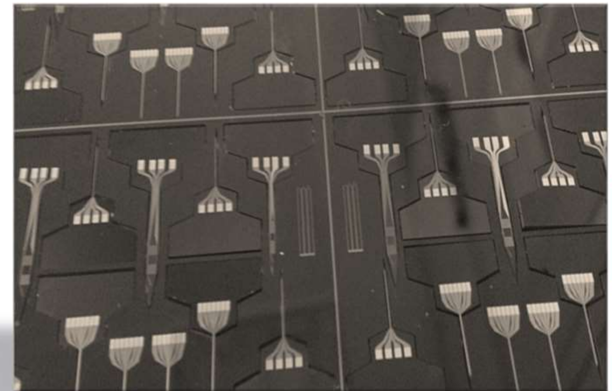

Needle sensors
Flexible MR Sensors

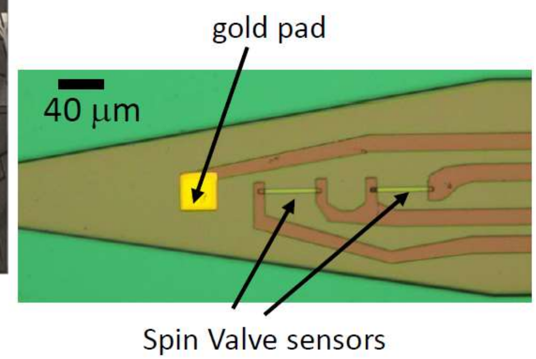

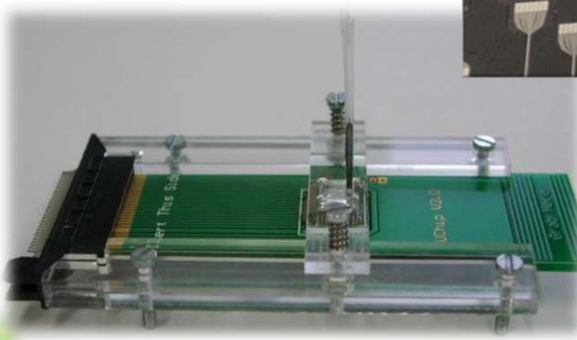

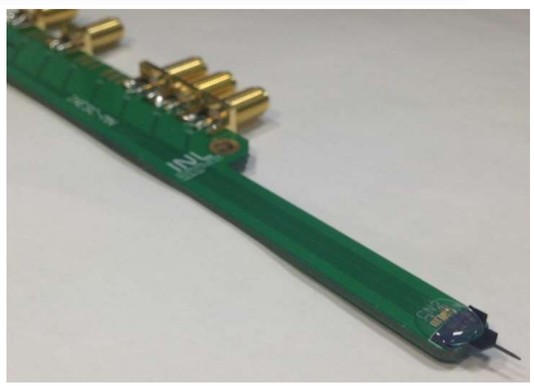

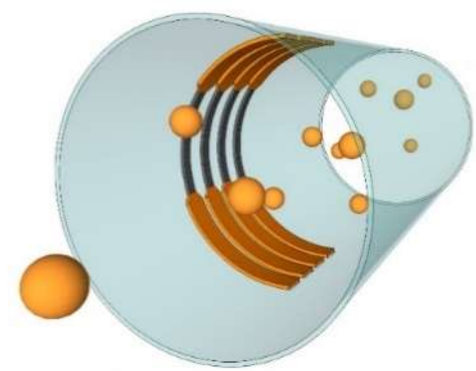

If no time: move to

Magnetic trap

Magnetic force exerted on MNP: $\boldsymbol{F}_{mag} = \nabla\,(\boldsymbol{m}\,.\,\boldsymbol{B})$

magnetic moment $\boldsymbol{m}$, magnetic field $\boldsymbol{B}$

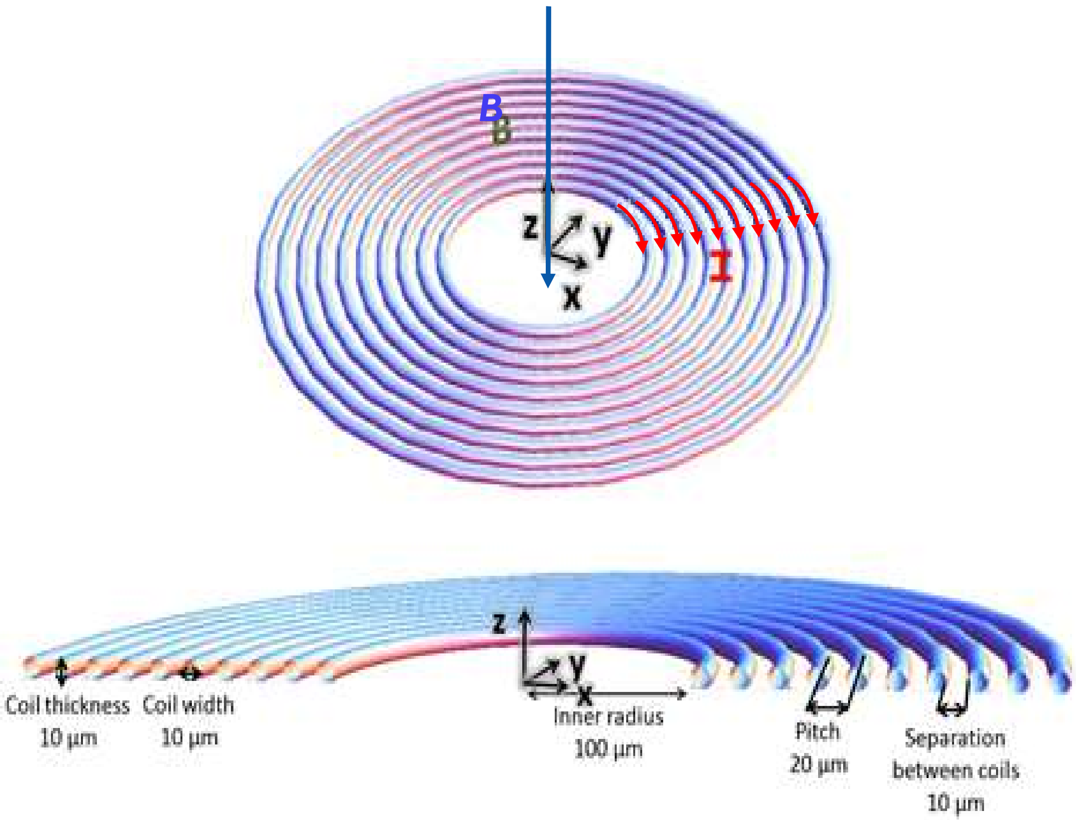

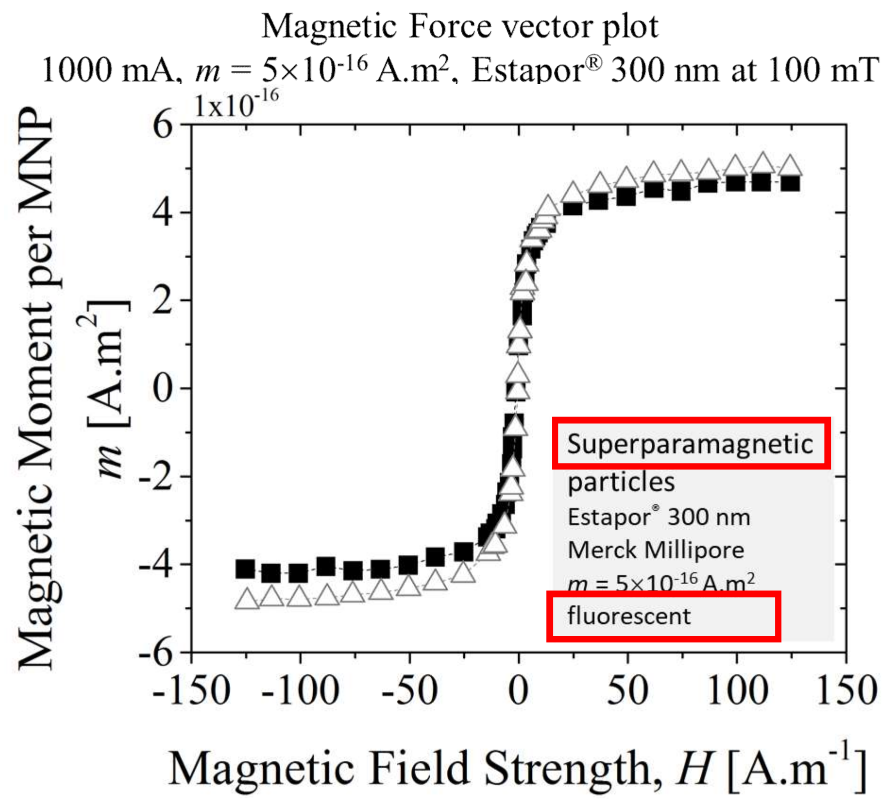

Microfabrication

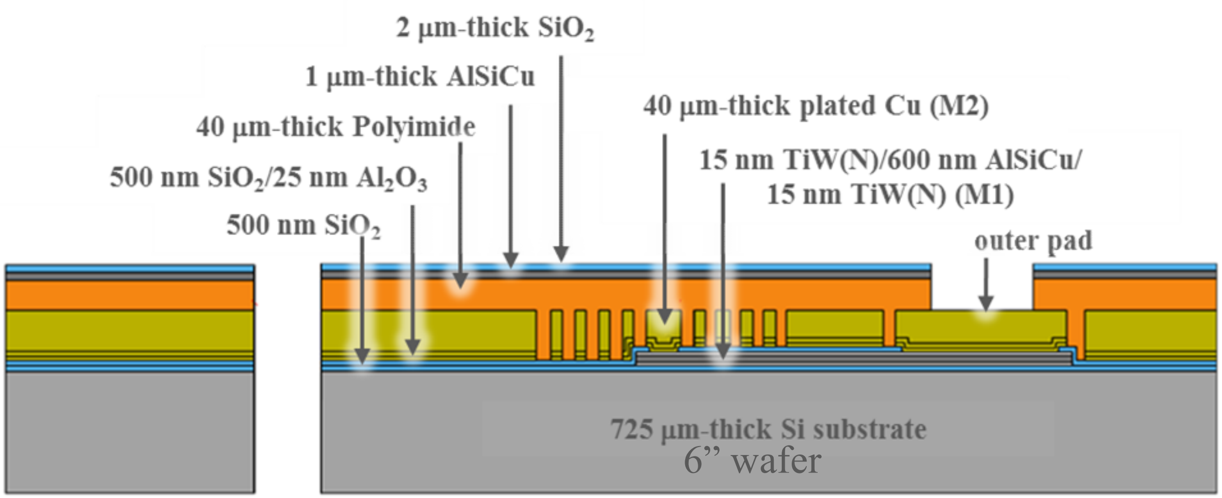

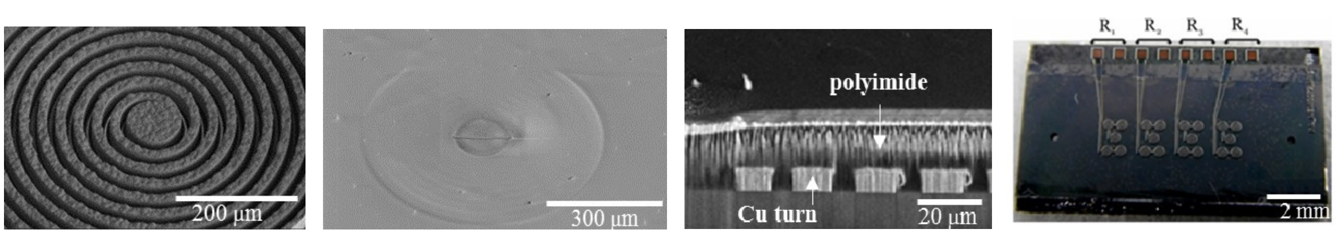

Silvério et.al., Micromachines 10(9):607 (2019);

Silverio et. Al., IEEE Trans Magn. 53 (11) 5100806 (2017)

1. PECVD 500 nm SiO_2 : 6" wafer
2. magnetron sputtering 15 nm TiW(N)/600 nm AlSiCu/15 nm TiW(N) : bottom electrode (M1 layer)
3. optical lithography
4. etching
   - This M1 film also connects the center of the coils to the contact pad
5. RF sputtering SiO_2 500 nm /Al_2O_3 25 nm
   - passivation layer to insulate the coil from the bottom electrode
6. optical lithography
7. electroplating 40 µm of Cu (M2 layer)
8. spin coating 40 µm polyimide
   - passivation
9. sputtering 1 µm AlSiCu
   - ensures an optimum optical contrast for the detection of the fluorescence in the MNP
10. sputtering 2 µm SiO_2
    - guarantees the planar surface required for the magnetic trapping and in the future, to promote probe linking
11. RIE to open 250 µm wide vias for contact pads

Magnetic Field Mapping

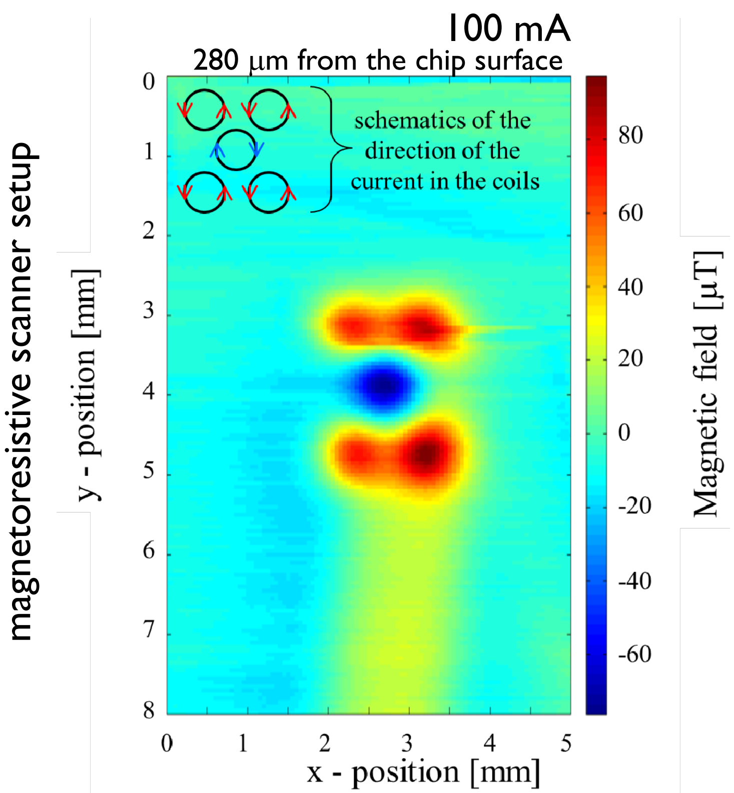

Magnetic Tunnel Junction (MTJ), sensitivity 0.04 V.mT^{-1}, dimension 91 × 14.5 μm^2

The vertical magnetic field over the **central coil** is **opposite** to the vertical field in the **4 outer coils**

- favorable for particle trapping and cell concentration

The field generated by 100 mA was measured to range between -70 to +90 μT

1000 mA actuation + PM field

- larger magnetic fields: -1500 to +3000 μT
- sufficient to generate a magnetic force to deflect the MNP trajectories and trap them

Thermal response

- Joule heating → flow cooling

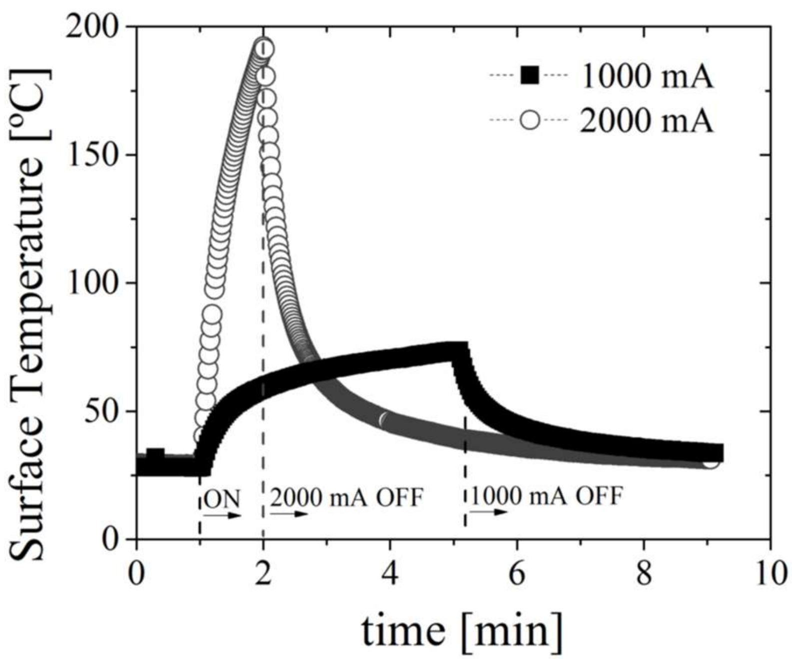

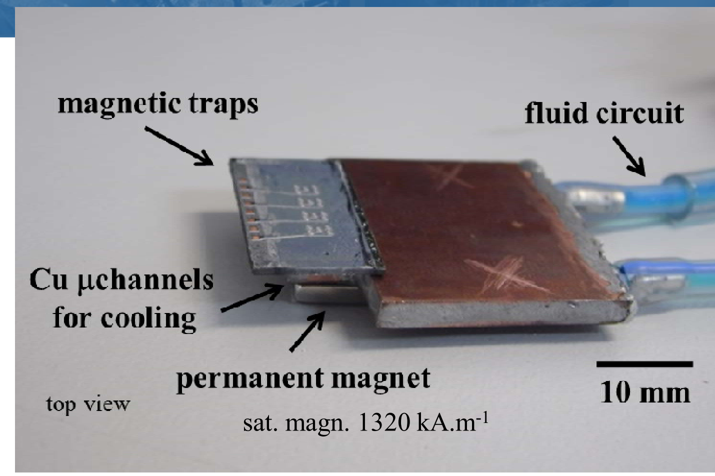

200 μm deep triangular microchannels enclosed on the copper block

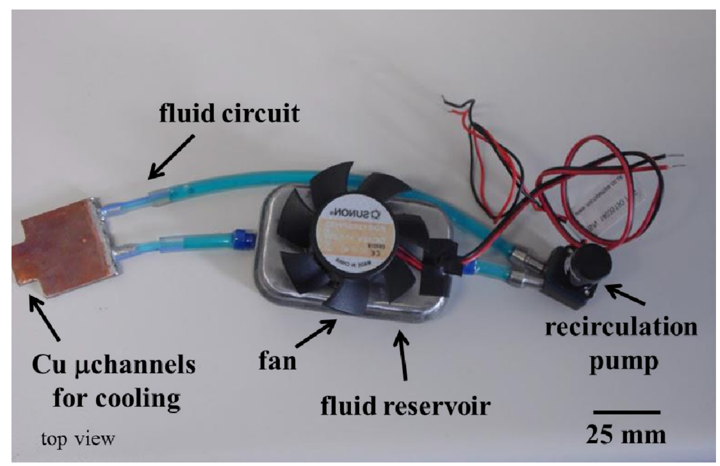

Silvério et.al., Micromachines 10(9):607 (2019);

Silverio et. Al., IEEE Trans Magn. 53 (11) 5100806 (2017)

Thermal response

pulsed current: 500 mA

8 s ON / 15 s OFF

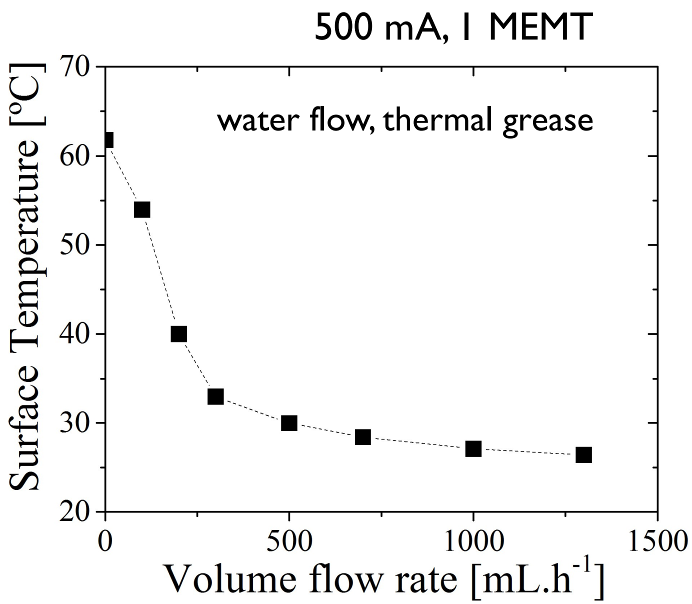

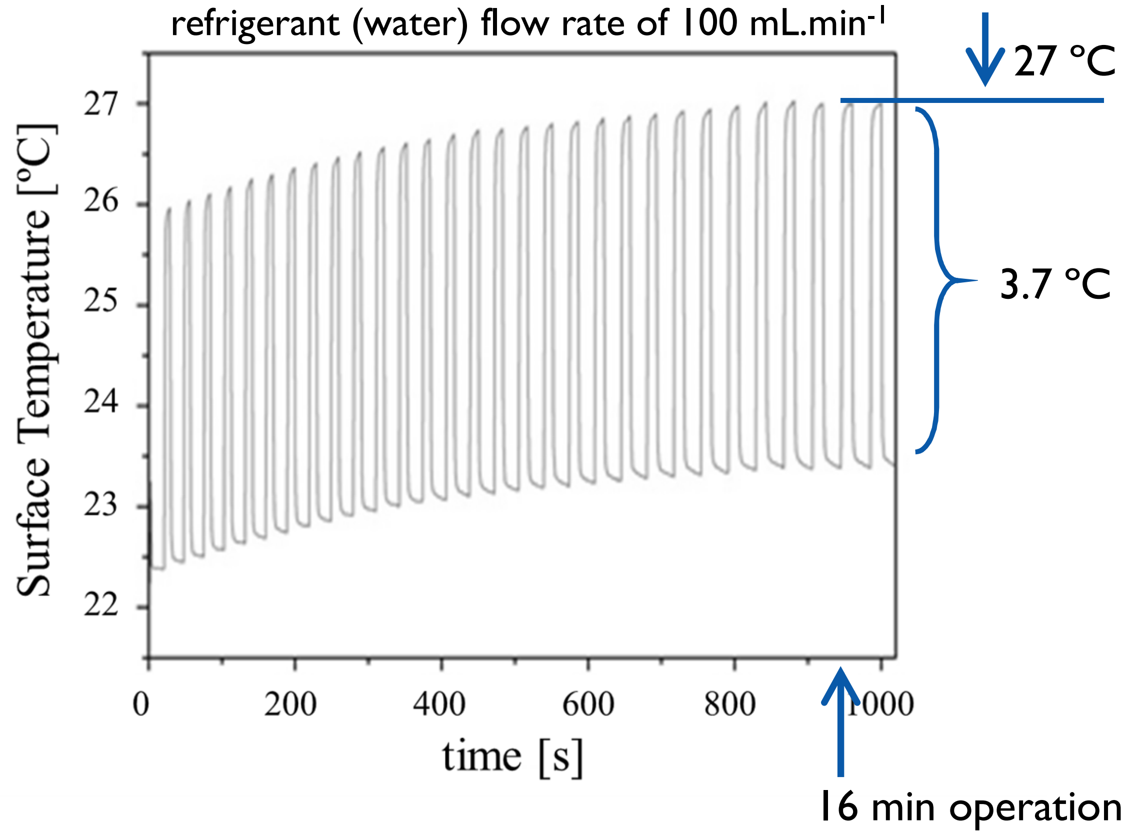

Silvério et.al., Micromachines 10(9):607 (2019);

Silverio et. Al., IEEE Trans Magn. 53 (11) 5100806 (2017)

Tombelli, et.al., Analytical and Bioanalytical Chemistry 414 (10), 3243 (2022)

MNP Trapping and concentration

16 pulses @ +750 mA

1 s ON + 2 s OFF + 1 s ON + …

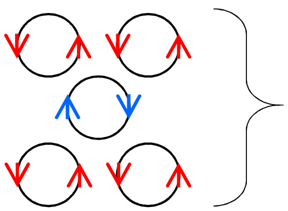

direction of the current in the coils

16 pulses @ –750 mA

1 s ON + 2 s OFF + 1 s ON + …

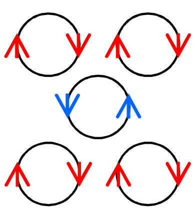

$T_{surf,max} = 3\ ^\circ C$

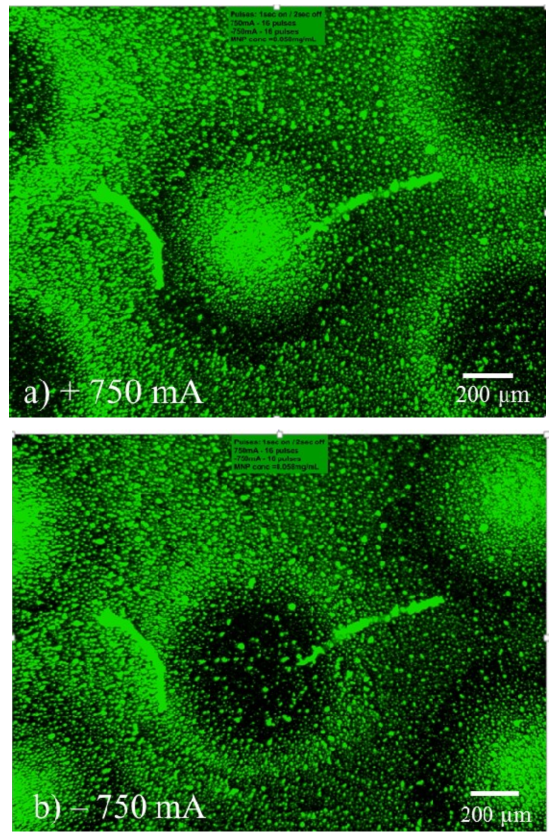

microchannel

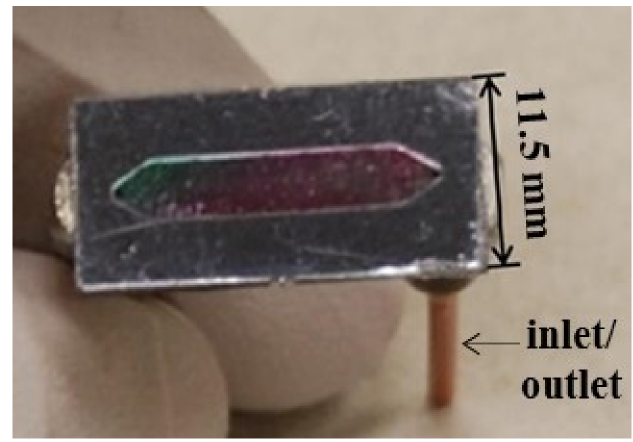

MNP concentration
0.058 mg.mL^{-1}

Silvério et.al., Micromachines 10(9):607 (2019);

Silverio et. Al., IEEE Trans Magn. 53 (11) 5100806 (2017)

Tombelli, et.al., Analytical and Bioanalytical Chemistry 414 (10), 3243 (2022)

Magnetic separation

volume magnetite

magnetic susceptibility (particle minus environment)

$$\mathbf{F}_{mag} \propto \frac{V_m \cdot \Delta\chi}{\mu_0} (\mathbf{B} \cdot \nabla)\mathbf{B}$$

magnetic field strength
magnetic field gradient

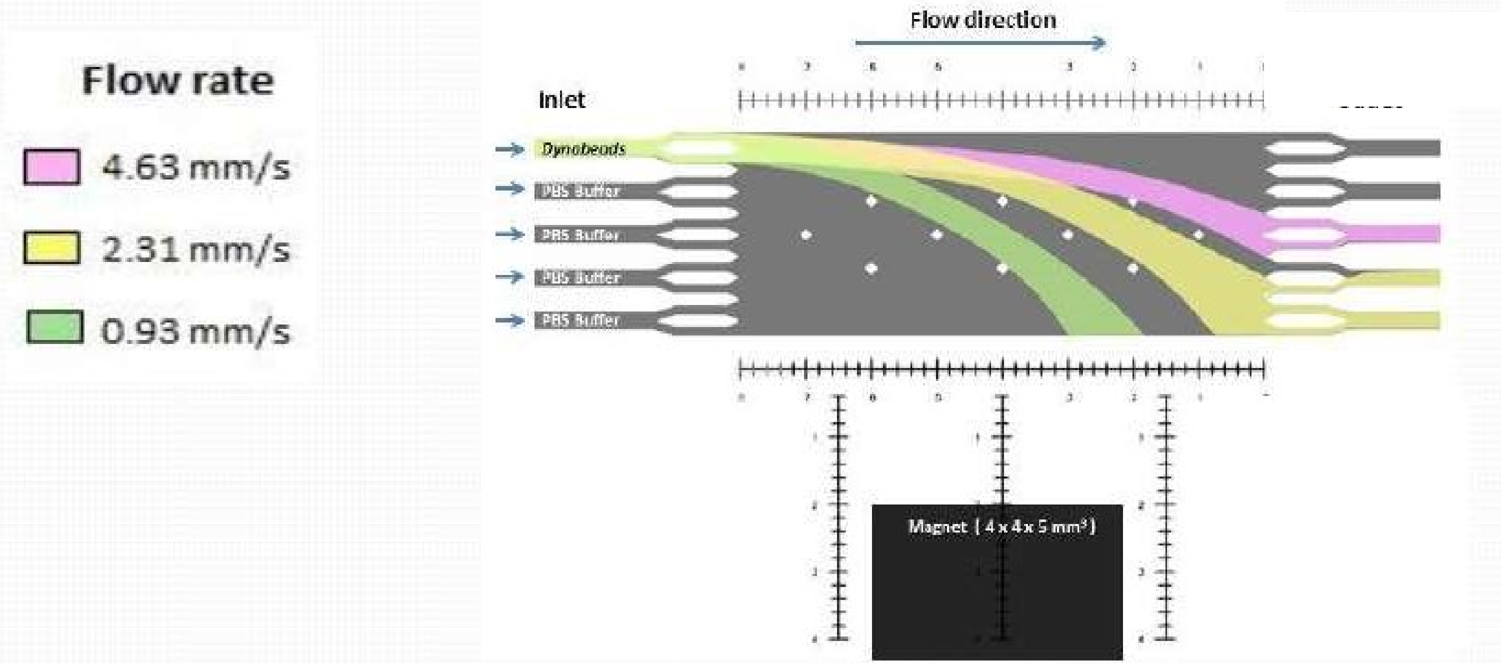

Tarn, Pamme, JMMM 2009, 4115.

Magnetic separation

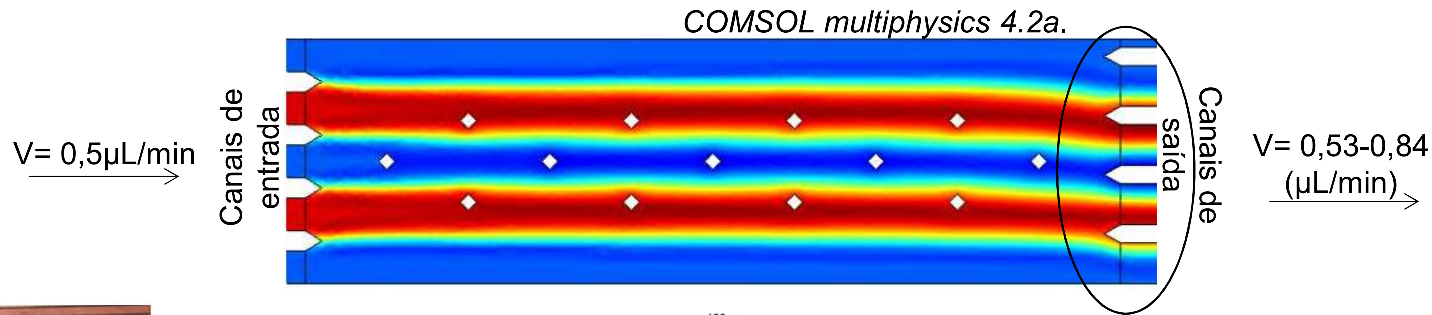

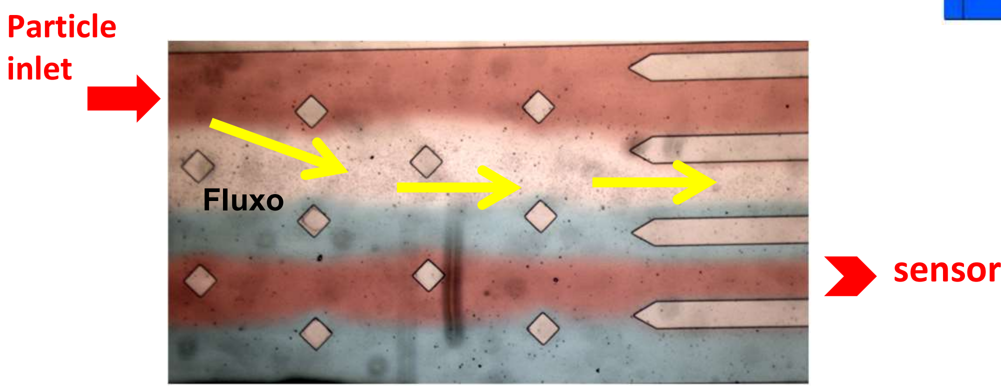

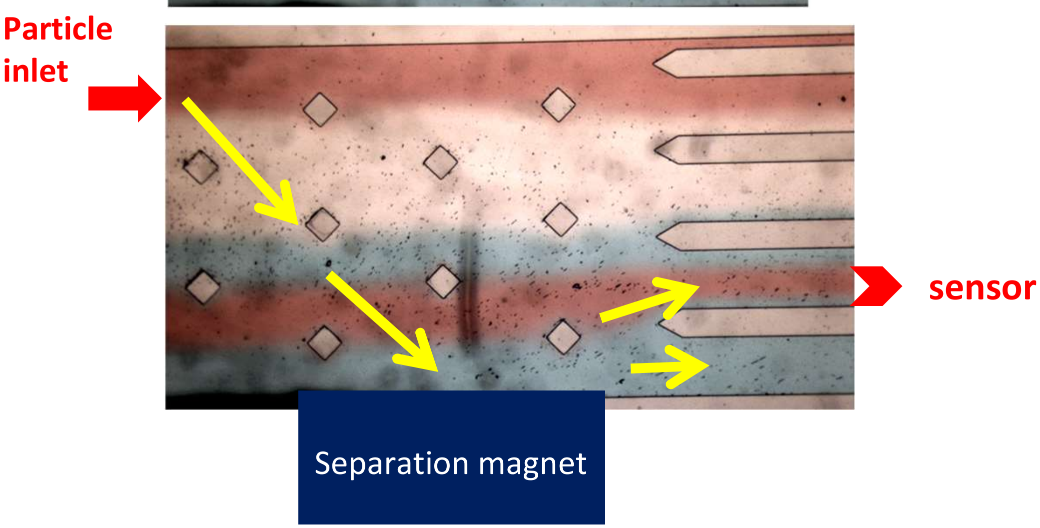

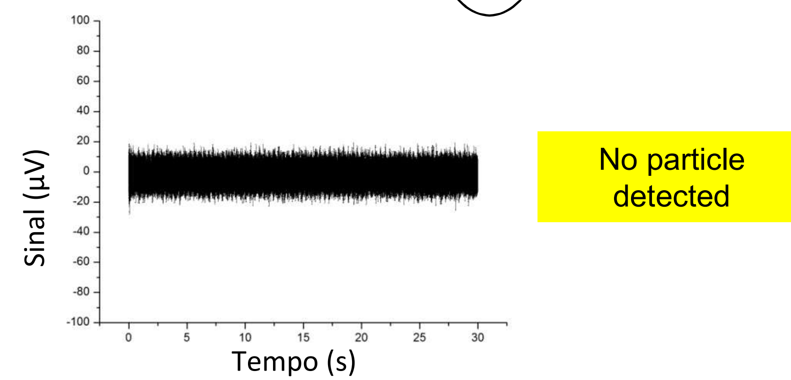

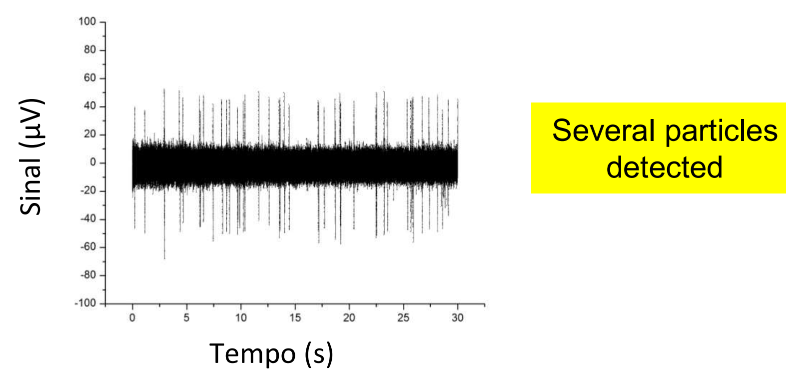

Magnetic biosensors

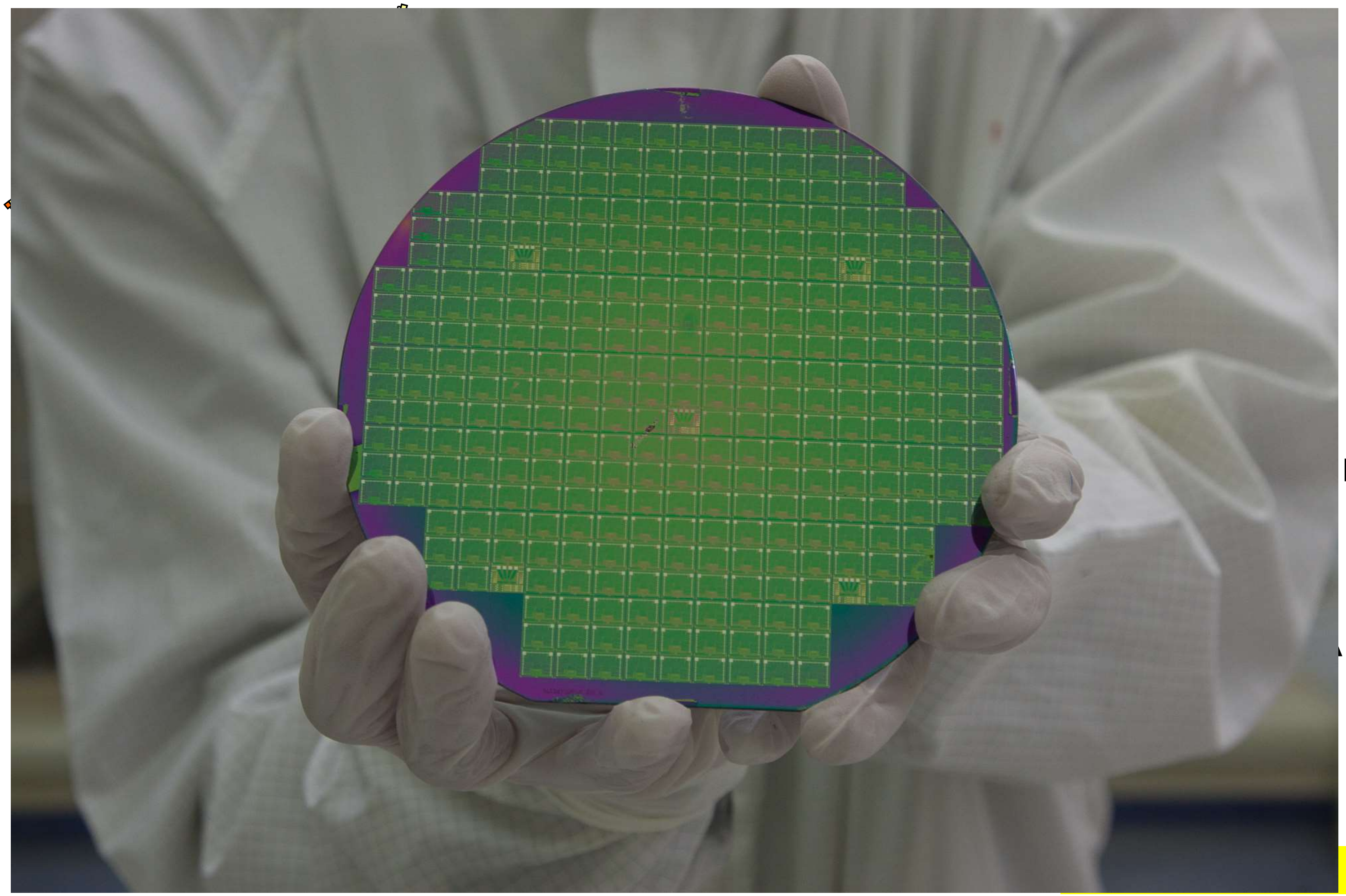

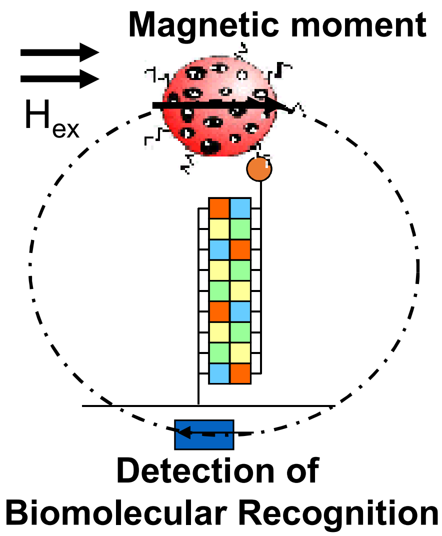

Biosensors and Bioelectronics, *210, 114302 (2022),*
Lab-on-Chip *18, 2593-2603 (2018);*
Trends in Biotechnology, August 2004
IEEE Magnetics Letters, *10 (1) (2019);*
Anal. Bioanal. Chem. *(2019) 411, pp. 1839 (2019);*
ACS Nano *11 (11), pp 10659–10664 (2017)*
Lab-on-Chip, 11 (13), 2255 – 2261 (2011)
Analytical Methods, ***8***, *119-128 (2016);*
Lab-on-Chip, 2012, 12 (3), 546 – 557 (2011)
Biosensors and Bioelectronics *11, 100149, (2022)*

INESC MN
Microsistemas e Nanotecnologias

Magnetic cytometer

INESC MN
Microsistemas & Nanotecnologias

Labels magnetization

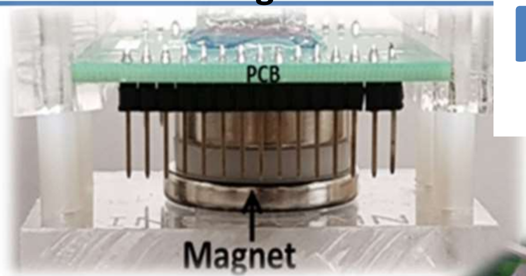

Detection principle

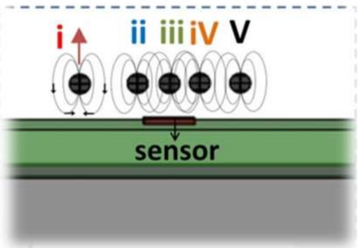

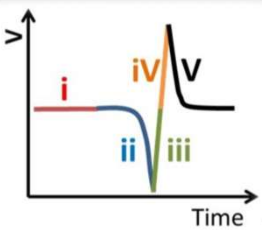

Time (s)

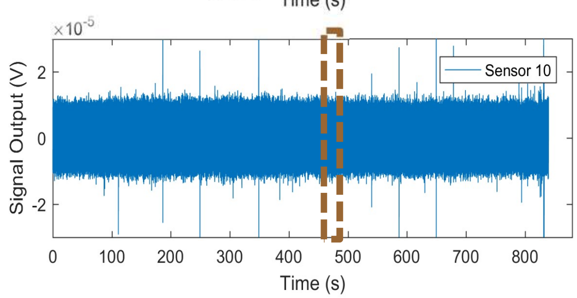

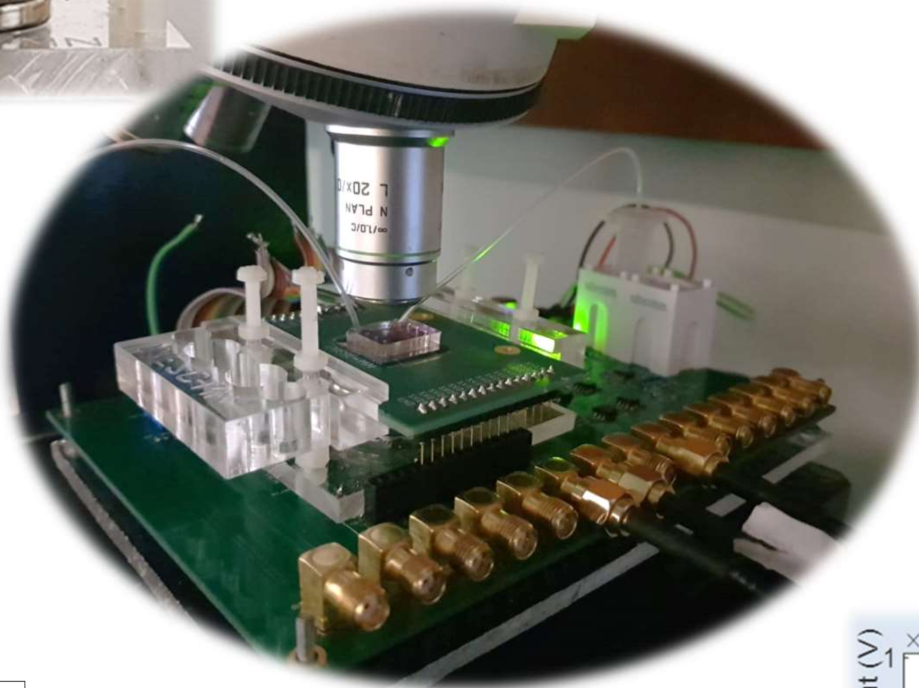

Microfluidics technology

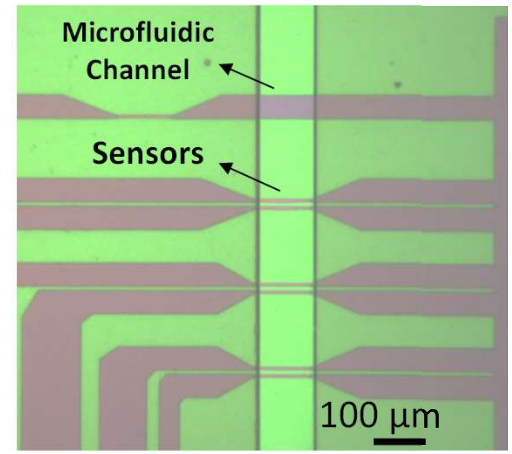

Detection signals

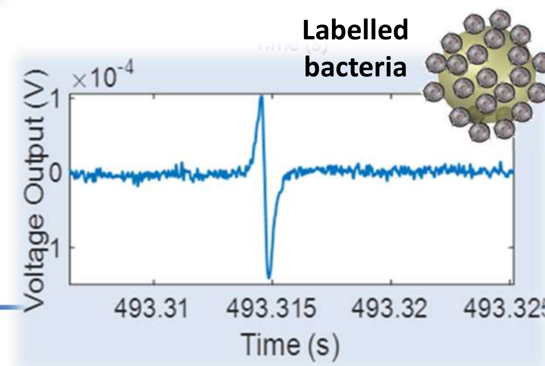

Lab-on-Chip, 11 (13), 2255 – 2261 (2011)

Freitas et.al., Lab-on-Chip, 2012, 12 (3), 546 – 557

Magnetic Labels

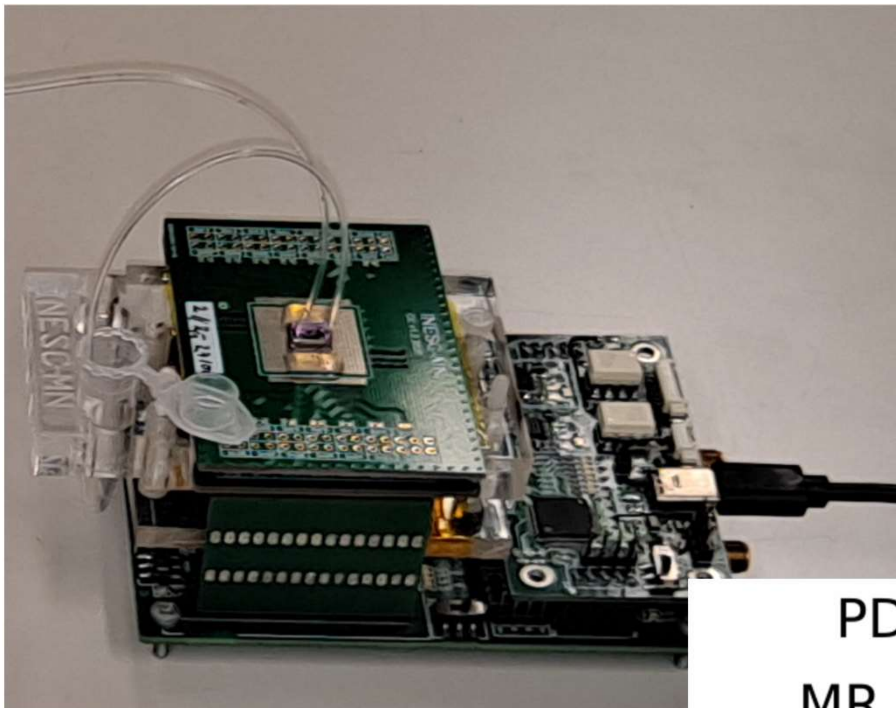

Particles typically used in bio-separation

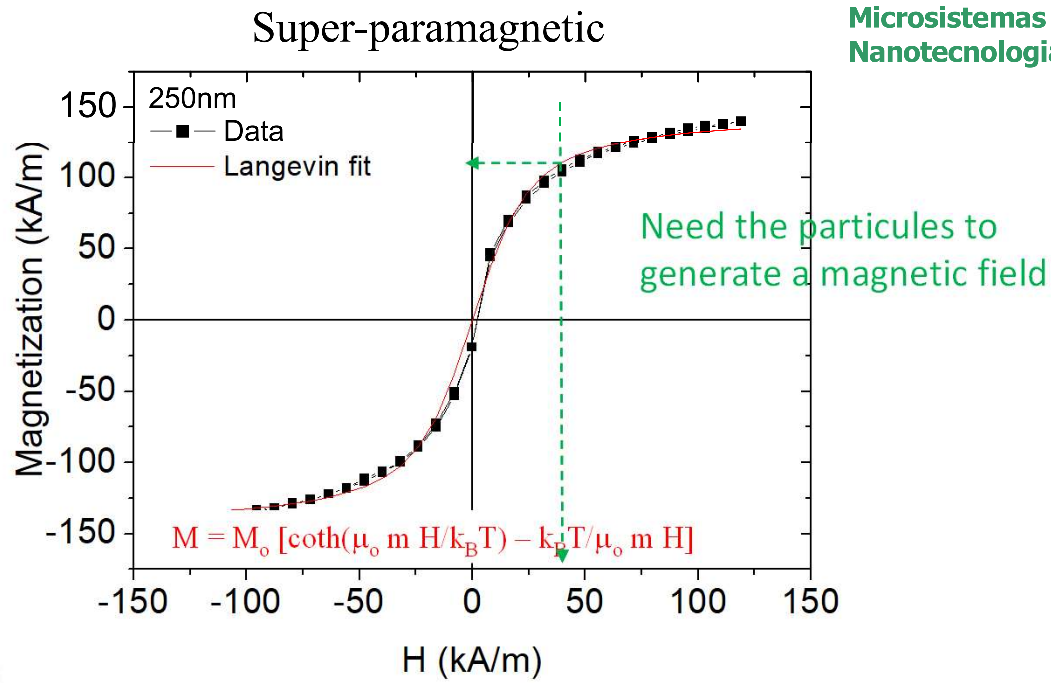

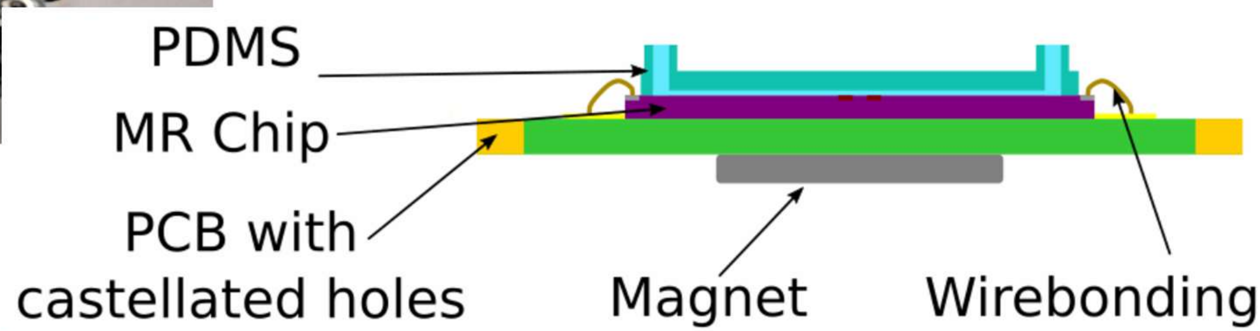

Lab-on-Chip, 11 (13), 2255 – 2261 (2011)
Freitas et.al., Lab-on-Chip, 2012, 12 (3), 546 – 557

Challenges – quantification

- **100nm magnetic particles** coated with protein A;
- **Rabbit α-goat Ab** → More affinity to protein A;
- **Goat α-*E.coli* Ab** → Already tested by IF;
- **Special SEM processing** without organic solvents;

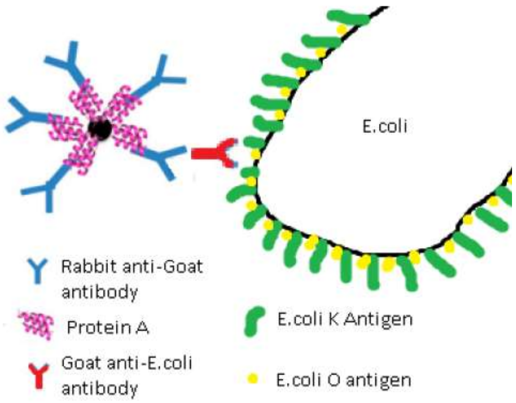

Adapted from Fernandes et.al. (2014)

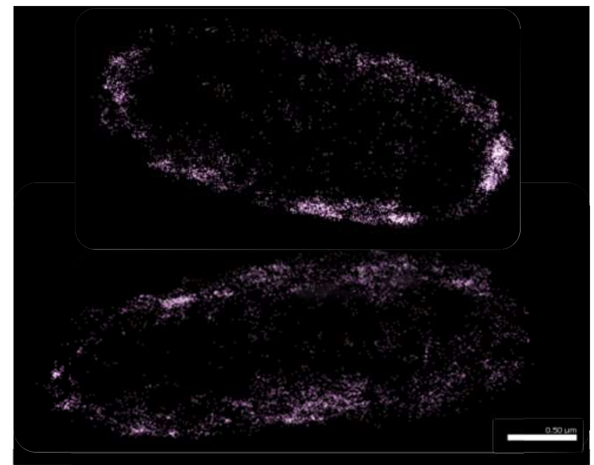

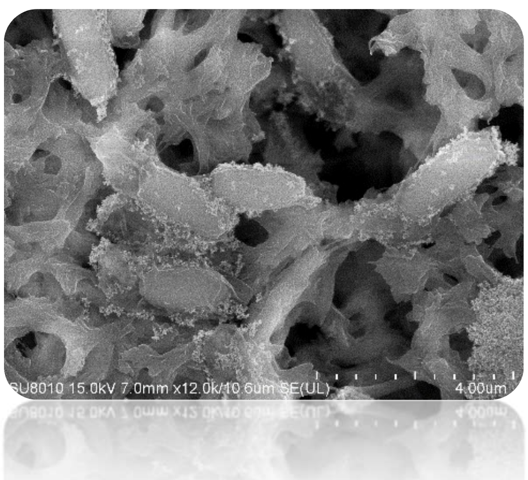

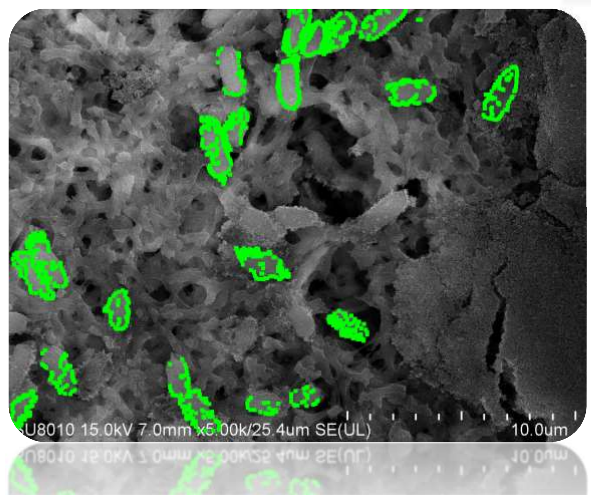

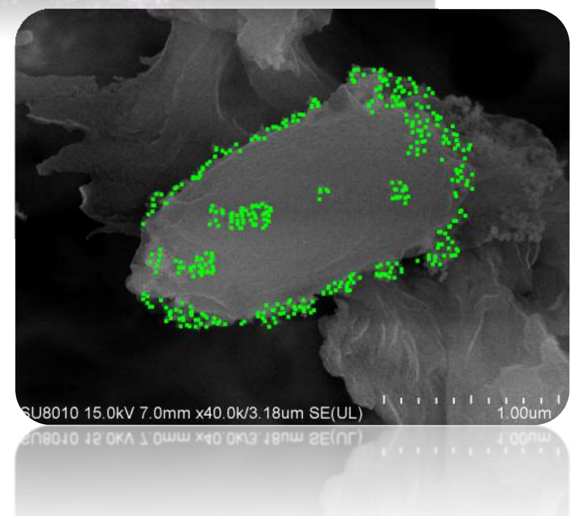

Contents lists available at ScienceDirect

Biosensors and Bioelectronics: X

journal homepage: www.journals.elsevier.com/biosensors-and-bioelectronics-x

INESC MN
Microsistemas & Nanotecnologias

On-site magnetic screening tool for rapid detection of hospital bacterial infections: Clinical study with *Klebsiella pneumoniae* cells

Ana R. Soares[a,b,*], R. Afonso[b,c], V.C. Martins[a], C. Palos[d], P. Pereira[d], Diogo M. Caetano[b,c], Davide Carta[a,b], S. Cardoso[a,b]

[a] Instituto de Engenharia de Sistemas E Computadores – Microsistemas e Nanotecnologias (INESC MN), Rua Alves Redol 9, 1000-029, Lisbon, Portugal
[b] Instituto Superior Técnico, Universidade de Lisboa, Av. Rovisco Pais 1, 1049-001, Lisbon, Portugal
[c] Instituto de Engenharia de Sistemas E Computadores - Investigação e Desenvolvimento, Rua Alves Redol 9, 1000-029, Lisbon, Portugal
[d] HBA – Hospital Beatriz Ângelo, Av. Carlos Teixeira 3, 2674-514, Loures, Portugal

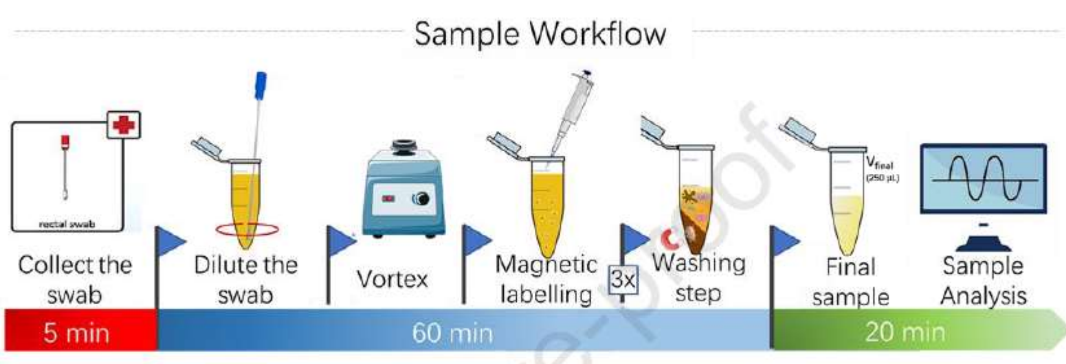

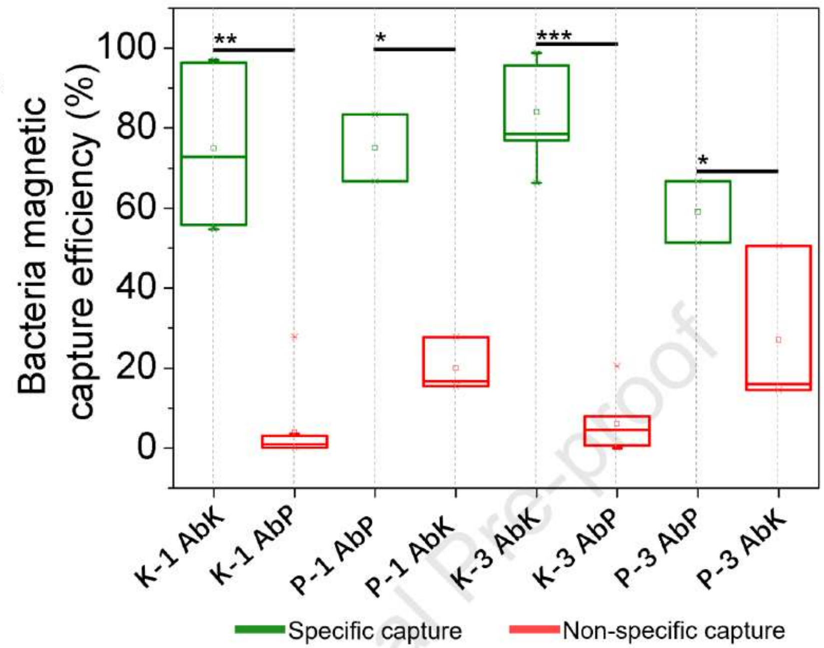

If no time: move to

Applications in scanners

If no time:
move to

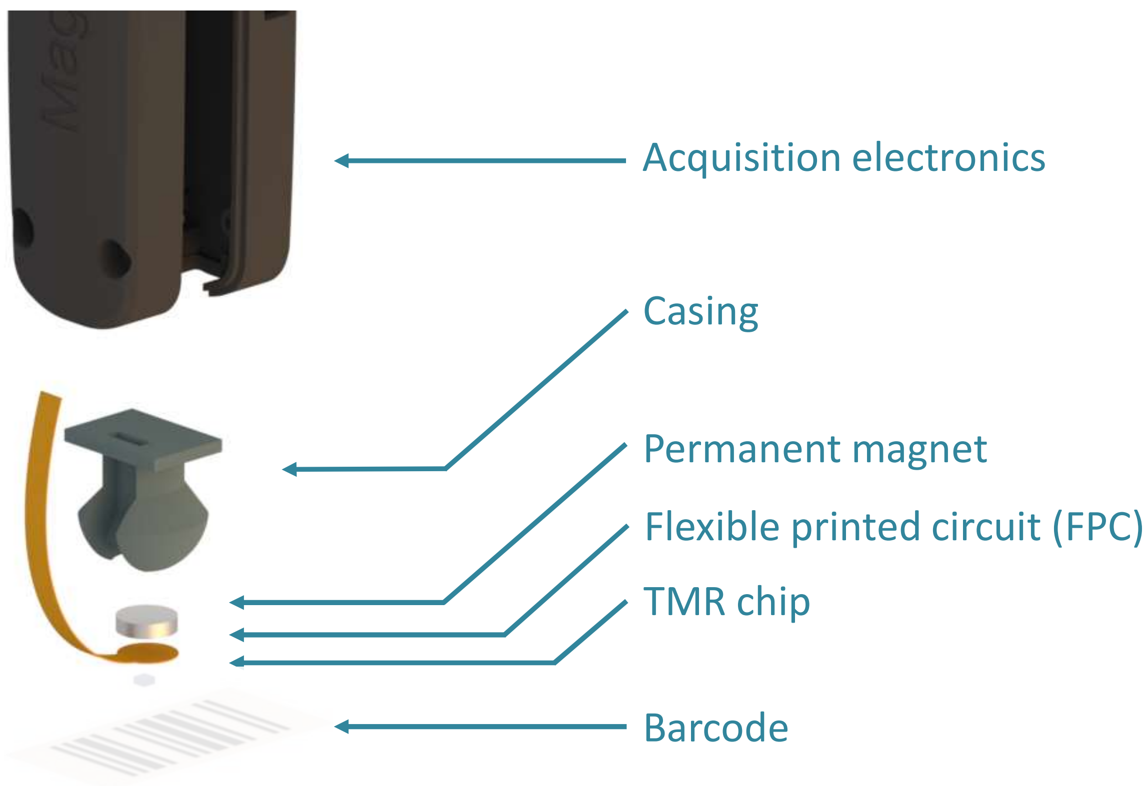
Acquisition electronics
Casing
Permanent magnet
Flexible printed circuit (FPC)
TMR chip
Barcode

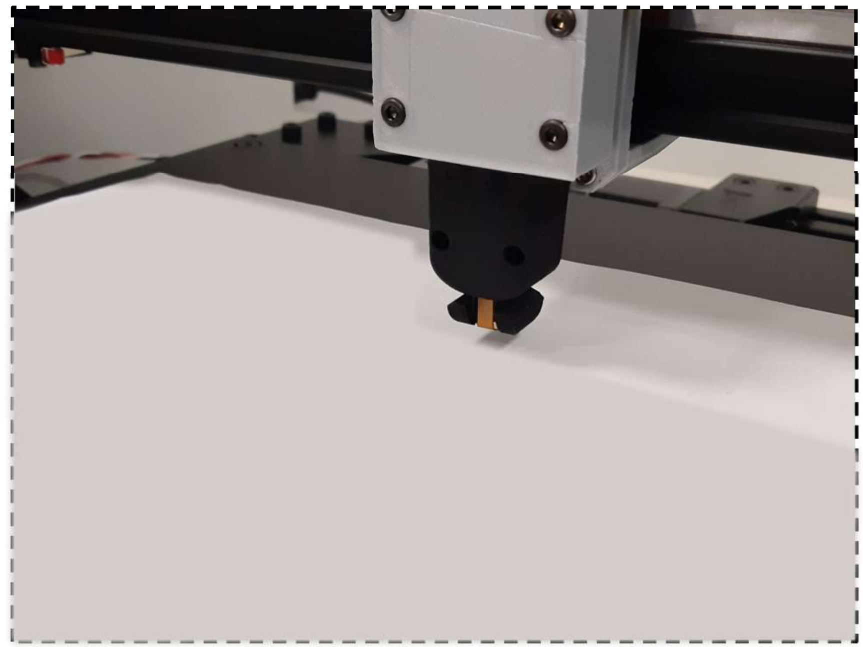

Swipe reader: printed barcode

INESC MN
Microsistemas e Nanotecnologias

Regular laserjet toners contain ferromagnetic (Fe_3O_4/Fe_2O_3) nanoparticles

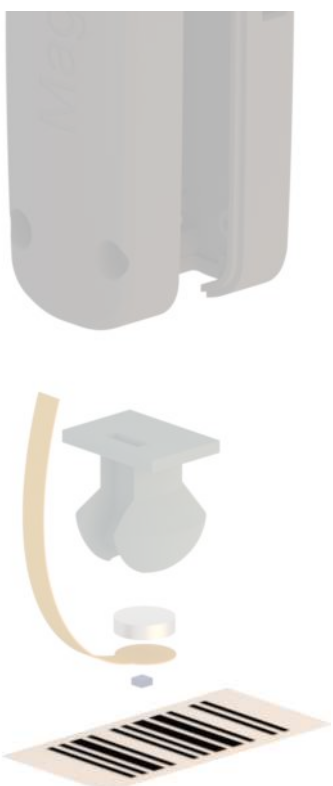

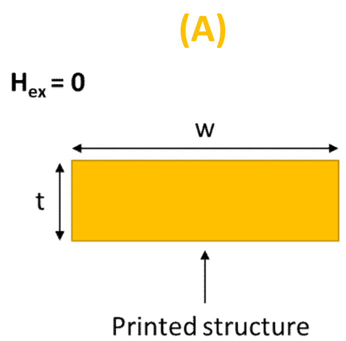

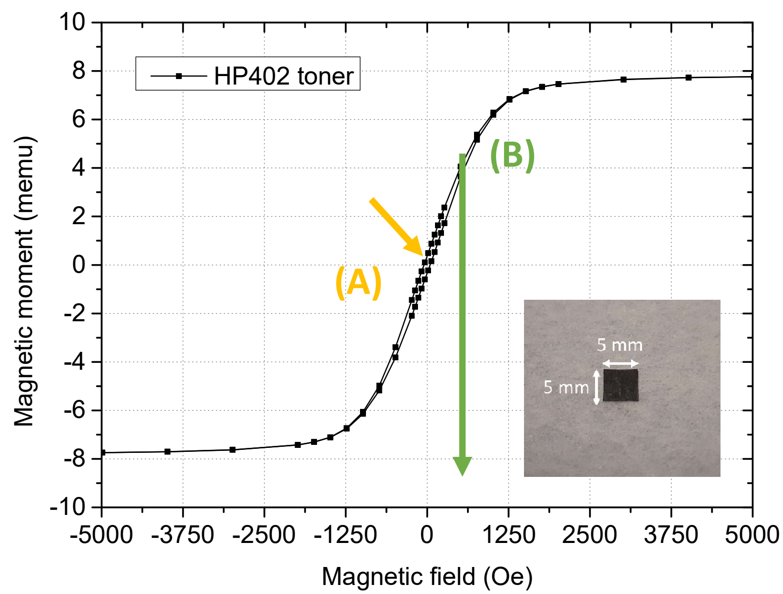

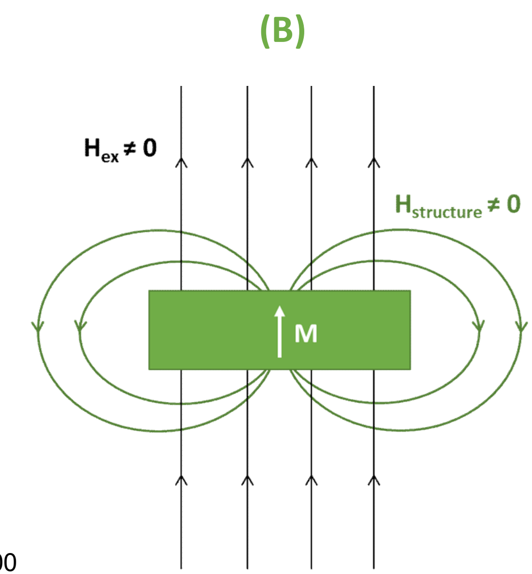

ferromagnetic material

→ Other toner/ink formulations also present ferromagnetic properties (e.g. MICR)

MagID

Alignment

Disc magnet provides a limited region where B < 1 mT (±170 µm) → **requires good accuracy from the alignment procedure**

No magnet

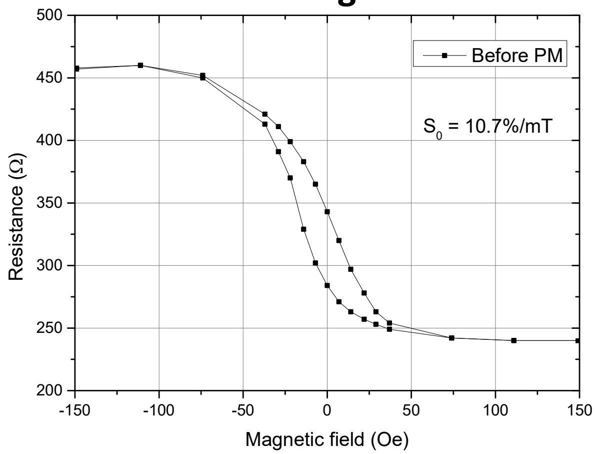

Poor alignment

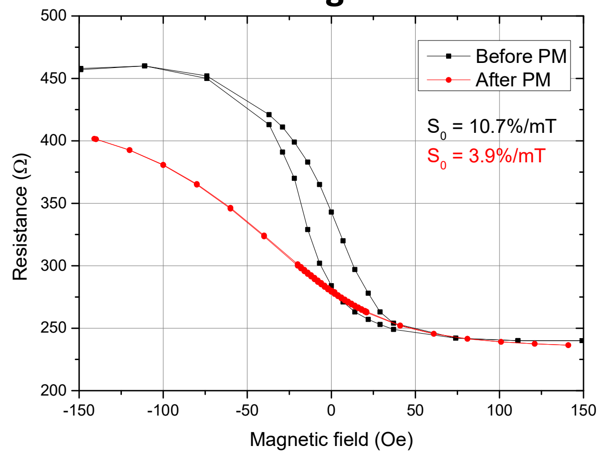

Good alignment

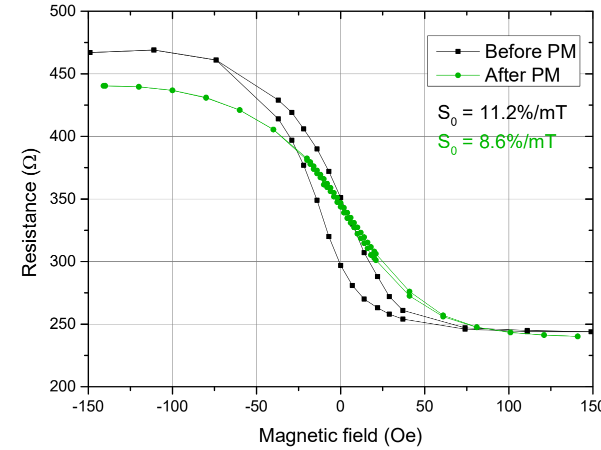

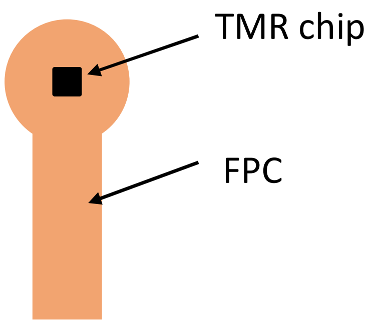

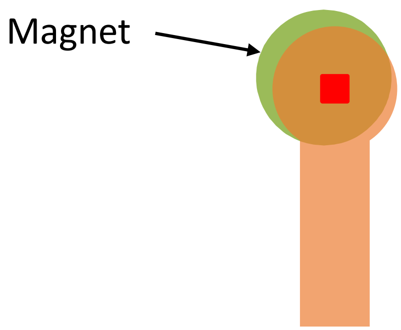

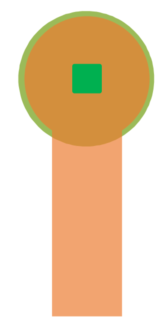

S.Abrunhosa. S.Cardoso, et.al
IEEE Trans. Magn. 58 (8), 4002304 (2022)

MagID | Project funded by the European Union | AIM | PD+F Programas de Doutoramento FCT | FCT Fundação para a Ciência e a Tecnologia

Swipe reader: assembly

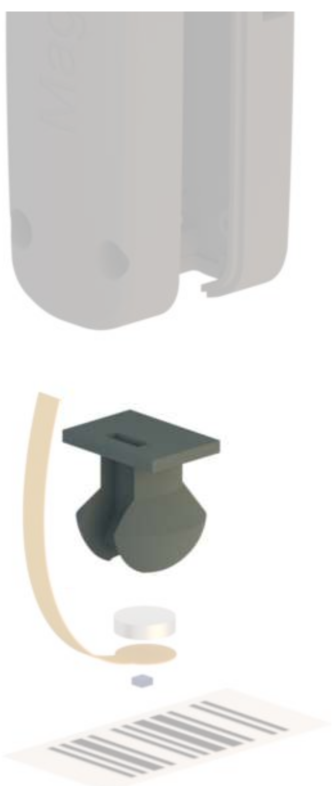

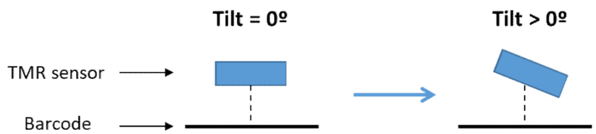

Purpose:

- Hold reader components
- Protect sensor chip
- Limit sensor tilt
- Minimise sensor-barcode distance

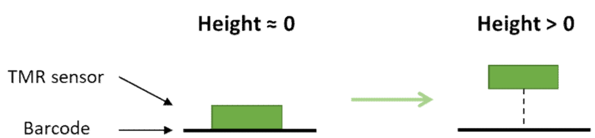

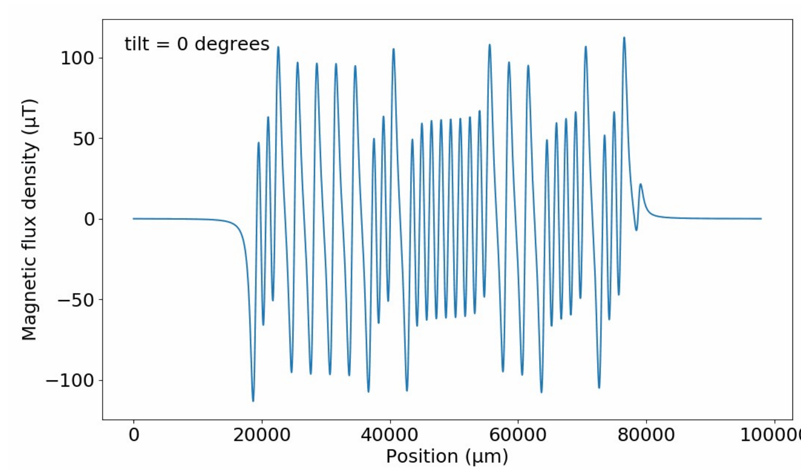

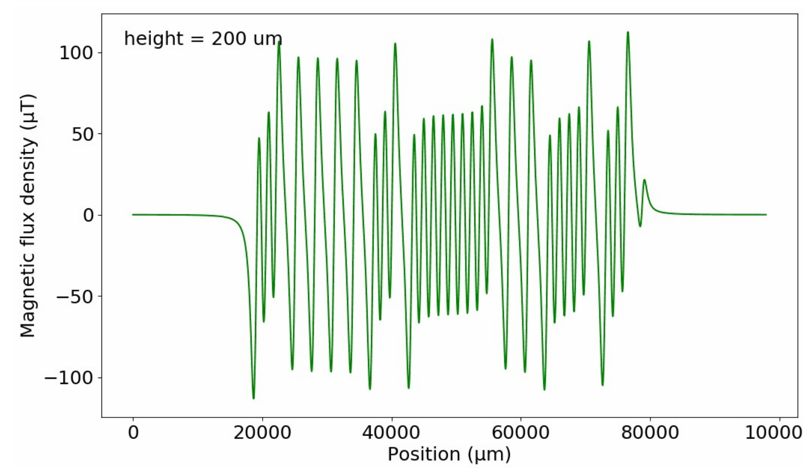

S.Abrunhosa. S.Cardoso, et.al
IEEE Trans. Magn. 58 (8), 4002304 (2022)

Handheld magnetic code reader

MagID

INESC MN
Microsistemas e Nanotecnologias

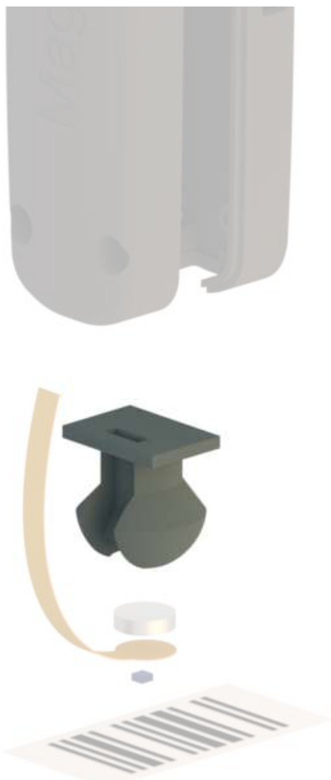

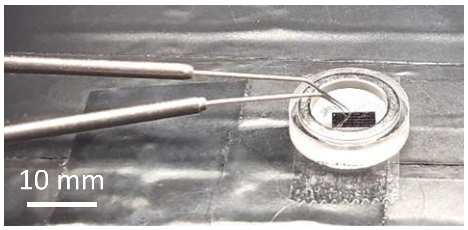

February 2020

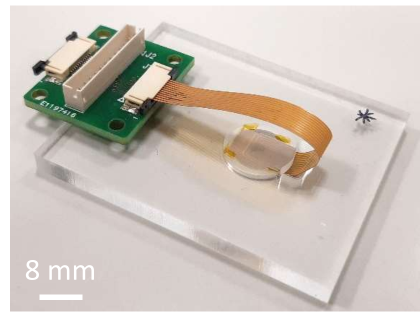

May 2020

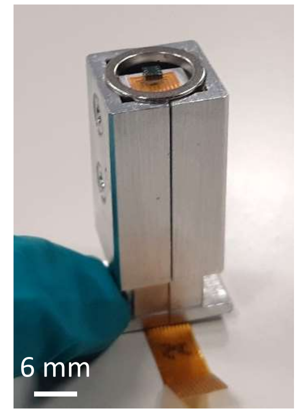

July 2020

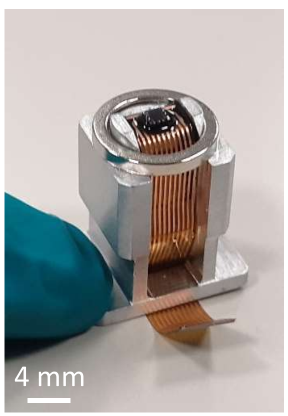

September 2020

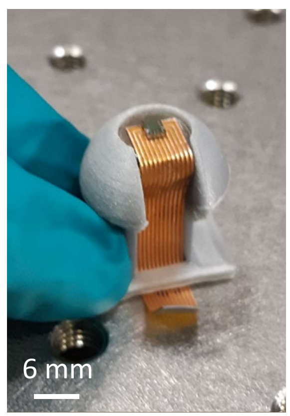

October 2020

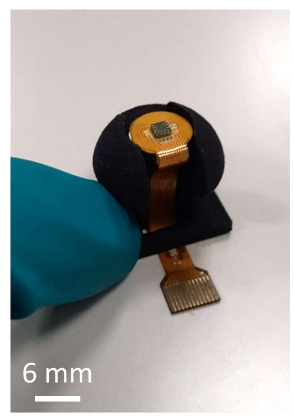

December 2020

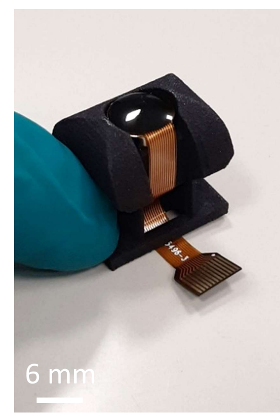

February 2021

...

Handheld magnetic code reader

MagID

INESC MN
Microsistemas &
Nanotecnologias

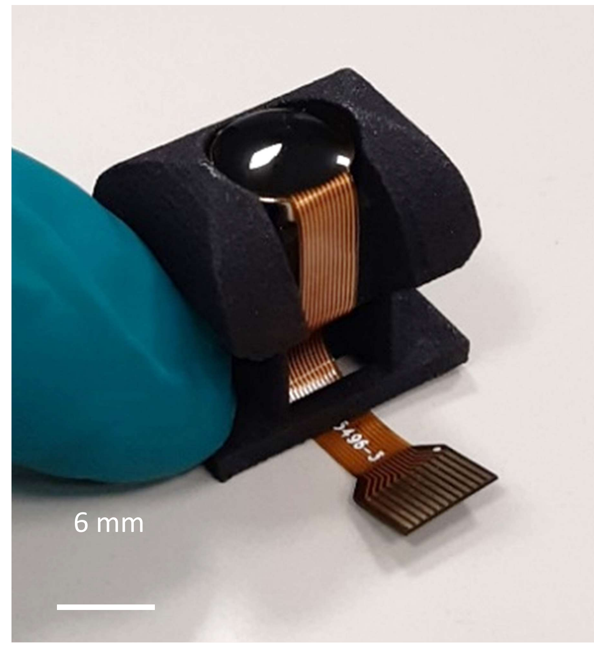

NEXT CHALLENGE:
Decode QR codes

Acknowledgments

To my team at INESC-MN (past and present)

IEEE MAGNETICS

INESC MN
Microsistemas & Nanotecnologias

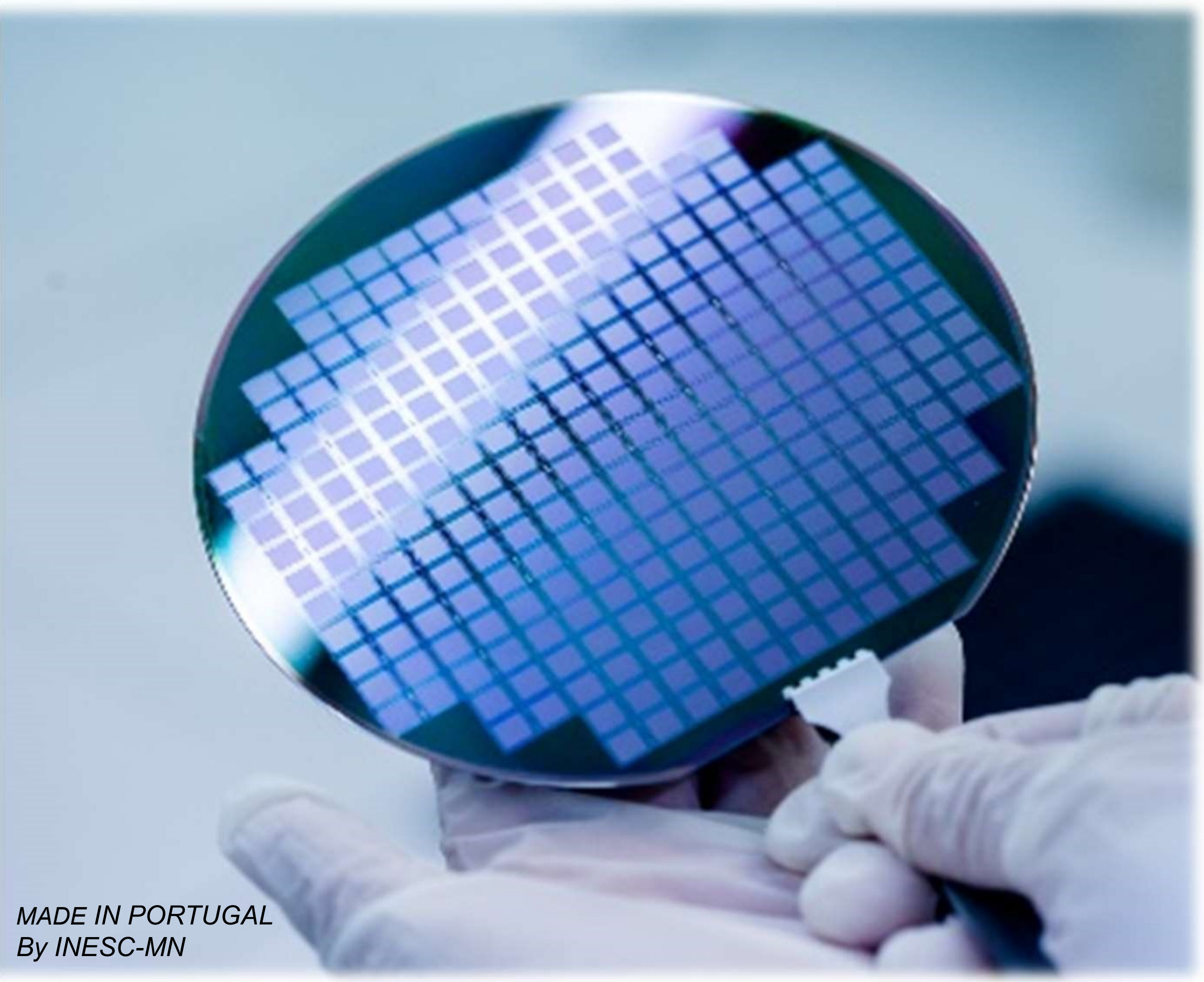

Contact for PhD, Post-Doc or internships:
scardoso@inesc-mn.pt

MISSÃO INTERFACE
AGÊNCIA NACIONAL DE INOVAÇÃO
REPÚBLICA PORTUGUESA
PRR Plano de Recuperação e Resiliência
Financiado pela União Europeia NextGenerationEU
IAPMEI
fct Fundação para a Ciência e a Tecnologia
inesc id lisboa
INL International Iberian Nanotechnology Laboratory
nffa.eu research infrastructure
AIM Advanced Integrated Microsystems

Mag-ID H2020-EIC-FTI-870017
MASMA H2020-EIC-SMEInst n. 858934
MagScopy4IHC LISBOA-01-0145-FEDER-031200